# Membrane electrode assemblies for PEM fuel cells: A review of functional graded design and optimization

Lei Xing[a,b*], Weidong Shi[c*], Huaneng Su[d], Qian Xu[d], Prodip K. Das [e], Baodong Mao[c], Keith Scott[e*]

a. Institute of Green Chemistry and Chemical Technology, Jiangsu University, Zhenjiang 212013, China

b. Department of Engineering Science, University of Oxford, OX1 3PJ, UK

c. School of Chemistry and Chemical Engineering, Jiangsu University, Zhenjiang 212013, China

d. Institute of Energy Research, Jiangsu University, Zhenjiang 212013, China

e. School of Engineering, Newcastle University, Newcastle NE1 7RU, UK

Corresponding authors:

Lei Xing (xinglei1314@gmail.com)

Weidong Shi (swd1978@ujs.edu.cn)

Keith Scott (k.scott@ncl.ac.uk)

## ABSTRACT

The use of platinum as a catalyst and the nonuniform distribution of current density inside a membrane electrode assembly result in high cost and low durability, which strongly hinders the wide adoption of proton exchange membrane fuel cells. For proton exchange membrane fuel cells operated at various loads, the required activities and mass transport rates are different because the reactant and product are nonuniformly distributed inside the membrane electrode assembly. Thus, a rational design for a membrane electrode assembly with a spatial distribution of functional components is helpful for reducing the usage of precious components, improving cell performance, and achieving uniform distributions of current density and heat. Herein, the graded design of the functional components in the gas diffusion layer, microporous layer, catalyst layer, and membrane along both the through-plane and in-plane directions within the membrane electrode assembly are reviewed for the purpose of reducing the cost and improving the performance and durability of proton exchange membrane fuel cells.

**Keywords**: PEM fuel cell, membrane electrode assembly, graded design, functional components, optimization

# 1. Introduction

Rapid industrialization and urbanization have led to an increased consumption of energy and serious global warming in the 21st century [1-4]. The carbon dioxide ($CO_2$) content in the atmosphere has increased by 30% since the industrial era began [5], of which approximately 17% came from the burning of fossil fuel in the internal combustion engines of vehicles [6]. Fossil fuels, as the main resources used to meet the global energy requirement, contribute to over 70% of the current world energy demand [7]. This eventually resulted in the depletion of limited nonrenewable resources, e.g., coal, oil and natural gas, and led to serious environmental pollution. It is clear that by 2050 oil and gas supplies will not be able to meet the global energy demand [8]. As a clean energy device using renewable resources as reactants, a fuel cell is considered an alternative and promising solution that is capable of improving the efficiency of energy utilization and reducing the emissions of greenhouse gases. Due to its higher energy-conversion efficiency and zero-emission potential, hydrogen-based proton exchange membrane fuel cells (PEMs) create a possibility of transforming the heavy carbon footprint-based economy into a sustainable carbon-free future [9-12].

As shown in Fig. 1, a typical PEM fuel cell unit includes a membrane electrode assembly (MEA) sandwiched between the flow field plates (FFPs) of the anode and cathode, into which flow channels are grooved. The MEA includes gas diffusion layers (GDLs) and catalyst layers (CLs) on the anode and cathode side, respectively, and a proton exchange membrane (PEM) in between. For better water management, the microporous layer (MPL) is commonly sandwiched between the GDL and CL. Typically, the CL, GDL and MPL are porous media with different components and structures used to deliver various functionalities. As an engine of the MEA, the oxygen reduction reaction (ORR) occurs inside the cathode CL, while hydrogen splits into protons and electrons at the anode CL. A proton migrates through the PEM, and electrons are transported via an external cycle from the anode to the cathode, where they combine with oxygen to produce water at the cathode. As a CL support, the GDL is a porous medium used for effective transport of electrons and heat, as well as of reactants and products in

the gas and liquid phases. The MPL is a more hydrophobic and compact layer used to maintain a hydrated membrane and mitigate water flooding inside the CL and GDL.

The process occurring inside the porous electrode constitute a fully coupled reaction-diffusion process. The reactant gases must be transported through the void space within the porous media and reach the active sites for electrochemical reaction. Meanwhile, an electrolyte polymer (Nafion ionomer) network and carbon matrix provide pathways for proton and electron migration, respectively. Due to the competitive relationship between the electrochemical reaction and effective species transport [13], optimal cell performance requires a different spatial distribution of the electrode compositions. Inside the MEA, the transport rates of electrons, ions and gases are altered by the Pt/C, Nafion ionomer and void space, respectively. An improper design would lead to a portion of the noble catalyst particles, e.g., those located at the inner CL close to the membrane, being insufficiently utilized due to the limitation of species transport, leading to a waste of precious catalyst. The optimal parameters for maximized cell performance, such as platinum and ionomer loadings and the porosity and hydrophobicity of the GDL, CL and MPL, vary according to the different operational requirement of PEM fuel cells. Therefore, the design of a functionally graded electrode is a promising strategy for cost reduction and performance optimization of the PEM fuel cells. Additionally, designs of functionally graded electrodes have been widely applied in high-temperature fuel cells [14-18].

To the best knowledge of the authors, there have been about a hundred published papers focusing on graded designs of PEM fuel cells. These studies include graded platinum and ionomers in the CLs, graded PTFE loading and porosity inside the GDL, graded hydrophobicity of the MPL and graded sulfonic acid within the PEM. Although many experimental and numerical studies have been intensively carried out, the optimal gradients of the functional components, e.g., the gradients of platinum within the CLs and porosity inside the MPLs, are still controversial due to their significant dependency on the operating conditions and model assumptions. In this paper, we review up-to-date research of graded electrode and membrane designs and summarize the optimal distributions of the corresponding functional components

within the GDL, CL, MPL and Nafion membrane under different operating conditions and assumptions. The anisotropic transport properties of gas, electrons, ions and heat along the through-plane (along the thickness direction of the porous media) and in-plane (along the gas flow direction parallel to the electrode surface) directions are elucidated. For accuracy of the PEM fuel cell models, the importance of the anisotropic properties of the MEA is emphasized. Then, the graded distribution of the porosity, hydrophobicity, platinum loading, ionomer loading of porous media and the density of the sulfonic acid group of the Nafion membrane are summarized. The optimal gradients of different design parameters are compared under different operating conditions. The multivariable optimization is discussed in the end. This review paper aims to share with readers a promising strategy for reducing the usage of precious Pt-based catalysts without sacrificing cell performance, with the help of a graded design of functional components and the optimization of their distributions within the MEAs. The functional graded design is capable of accelerating the commercialization and industrialization of PEM fuel cell technology.

# 2. Anisotropic Properties

As a key component of the MEA, the porous electrodes, including the GDL, MPL and CL, are typically prepared from highly porous carbon fiber materials, e.g., carbon paper or cloth. Due to the special constitutive orientations of carbon fibers, the porous electrodes exhibit strong structural anisotropy, which consequently leads to variations of the transport properties, such as the electrical resistance [19-21], thermal conductivity [22, 23], species diffusivity [24, 25] and electrode permeability [26-28], along both the through-plane and in-plane directions. In addition, according to the theory of numerous previous studies [29-31], the capillary diffusivity is a function of the electrode permeability. Therefore, anisotropic liquid water transport through porous electrodes under a capillary mechanism is initiated by the anisotropic permeability of the electrode.

The rate of gas transport through a porous electrode is characterized by its effective diffusivity, which is a function of the electrode porosity and tortuosity and the intrinsic diffusion coefficient of each

individual species in a gas mixture. Due to the formation of water, the electrode porosity is reduced. Considering the anisotropy of the microchannels as a gas transport pathway within the electrodes, the effective diffusivity of species, $D_i^{eff}$, in a porous media containing random fibrous materials has to be corrected by the percolation theory [32, 33] as follows:

$$D_i^{eff} = \begin{cases} (1-s)^{1.5}\varepsilon_p\left(\dfrac{\varepsilon_p-\varepsilon_{pc}}{1-\varepsilon_{pc}}\right)^{0.521} D_{i,g}^0 & in-plane \\ (1-s)^{1.5}\varepsilon_p\left(\dfrac{\varepsilon_p-\varepsilon_{pc}}{1-\varepsilon_{pc}}\right)^{0.785} D_{i,g}^0 & through-plane \end{cases} \quad (1)$$

where $s$ is the liquid water saturation, $D_{i,g}^0$ ($m^2\ s^{-1}$) is the intrinsic diffusion coefficient of gas species, *i*, and $\varepsilon_p$ is the porosity of the electrode. $\varepsilon_{pc}$ is the percolation critical value of porosity, which equals 0.11 as reported in Ref. [24].

The anisotropic electrode permeability for gas transport, $k_p^{eff}$, is expressed as follows [34, 35]:

$$k_p^{eff} = \begin{cases} \dfrac{R^2\varepsilon_p(\varepsilon_p-\varepsilon_{pc})^{2.521}}{8(\ln\varepsilon_p)^2(1-\varepsilon_p)^{0.521}(1.521\varepsilon_p-\varepsilon_{pc})^2}(\varepsilon_p)^{1.5} & in-plane \\ \dfrac{R^2\varepsilon_p(\varepsilon_p-\varepsilon_{pc})^{2.785}}{8(\ln\varepsilon_p)^2(1-\varepsilon_p)^{0.785}(1.785\varepsilon_p^0-\varepsilon_{pc})^2}(\varepsilon_p)^{1.5} & through-plane \end{cases} \quad (2)$$

where $R$ (m) is the radius of the carbon fiber.

The in-plane effective diffusion coefficient is typically higher compared to the through-plane effective diffusion coefficient due to the alignment of fibers, following the direction in which there are fewer blockages. As described by Nam and Kaviany [32], the change in electrode tortuosity for species transport along the through-plane direction is more significant with water droplet formation. Thus, the through-plane diffusivity is reduced more obviously in the presence of water due to the architectural variation of the electrode.

Heat management is also a crucial issue for PEM fuel cells due to its impact on the electrochemical reaction, species transport and saturation pressure of the vapor. The heat transport rate varies in different domains, e.g., in the bipolar plates, GDLs, CLs, and MPLs, in which the effective thermal conductivity strongly depends on the composition of the domain. Theoretically, the effective thermal conductivity is a function of the volume fractions and intrinsic thermal conductivities of the solid matrix, as well as the liquid water and gases present inside the void space of the porous electrode. Due to the anisotropic properties of the porous electrode, e.g., those of the carbon fibers and void space, the in-plane and through-plane thermal conductivity must be separately calculated and measured. The anisotropic effective thermal conductivity of the solid component of the electrode, $k_T^s$, can be expressed as follows [36]:

$$k_T^s = \begin{cases} 1-(\frac{3\varepsilon_p}{2+\varepsilon_p})0.977\exp[0.344(1-\varepsilon_p)](1-\varepsilon_p)^{-0.009}k_s^0 & in-plane \\ 1-(\frac{3\varepsilon_p}{2+\varepsilon_p})0.963\exp[0.881(1-\varepsilon_p)](1-\varepsilon_p)^{-0.008}k_s^0 & through-plane \end{cases} \quad (3)$$

where $k_s^0$ is the intrinsic thermal conductivity of the solid matrix within the electrode and depends upon the composition of the electrode.

Electron and proton transfer within the porous electrode rely on the carbon fiber and the developed ionomer network throughout the void space. The impact of the anisotropy of electron conductivity on the local current density distribution and overall cell performance have been intensively studied [19-21, 36]. As electron transport media, carbon fibers are normally oriented along the in-plane direction, resulting in a higher in-plane electrical conductivity (5000 - 23000 S $m^{-1}$) than through-plane conductivity (300 - 1400 S $m^{-1}$) [37-39]. The effective anisotropic electrical conductivity, $\sigma_s^{eff}$, is given as follows [35, 36]:

$$\sigma_s^{eff} = \begin{cases} \left[1-(\frac{3\varepsilon_p}{2+\varepsilon_p})0.962\exp[0.367(1-\varepsilon_p)](1-\varepsilon_p)^{-0.016}\right]\sigma_s^0 & in-plane \\ \left[1-(\frac{3\varepsilon_p}{2+\varepsilon_p})0.962\exp[0.889(1-\varepsilon_p)](1-\varepsilon_p)^{-0.007}\right]\sigma_s^0 & through-plane \end{cases} \quad (4)$$

where $\sigma_s^0$ (S m$^{-1}$) is the intrinsic electrical conductivity of the electrode.

Eqns. (1) – (4) are obtained from the percolation theory rather than the typical Bruggeman approximation, as it is widely used and provides a more accurate estimation of the effective transport properties.

The values of the studied parameters related to the in-plane properties typically exceed those of the through-plane case. The ratios of in-plane and through-plane parameters, including electrode permeability, gas and water diffusivities, and electrical, ionic and thermal conductivities, were compared and summarized in the work of Xing et al. [40]. It is indicated in Fig. 2. that the ratios are sensitive to the porosity of the porous media. It can be seen that the ratios are sensitive to the porosity of the porous media in that the ratios of the electron, ion, and thermal conductivities increase dramatically with the increase in the electrode porosity, whereas the ratios of the electrode permeability and gas and water diffusivities gradually decrease. The in-plane and through-plane ratios indicate the influence of the anisotropic transport properties on the transport rates of the associated processes, such as the diffusion rate of the reactant gas through the void space and the transport rates of electrons and ions via the carbon and ionomer network inside the porous electrode, showing the index of inaccuracy if the studied parameters are assumed to be isotropic.

Fig. 3 shows the effect of anisotropic mass diffusivity, as determined from the percolation theory, on the predicted current density under channel and land. A significant increase in the current density under land is observed, while the current density under the channel remains virtually unchanged. This can be explained by the deformation of the GDL under the clamping force of the bipolar plates. Owing to the immediate contact between the channel ribs and carbon papers, the deformation of the GDL is more significant under the land than under the channel. A GDL deformation leads to a decrease in porosity and an increase in the electron conductivity, which has a pronounced impact on the current density distribution at low and medium current densities. This indicates that the anisotropy of mass diffusivity and electrical conductivity may change the characteristics of overpotential and current density

distributions under the gas channels and land areas under certain conditions [22-24]. To achieve better fuel cell performance, the graded porous electrode needs to be carefully designed along both the in-plane and through-plane directions.

# 3. Graded GDL

The GDLs of PEM fuel cells are typically porous media of hundreds of micrometers in thickness. As a component of the MEA, the GDL is normally made of a woven carbon cloth or a nonwoven carbon paper. High electric conductivity, appropriate porosity, strong mechanical strength and good chemical stability are desirable properties. The role of the GDL is to support the CL and affect the diffusion of the reactant, water, heat and electrons [41-43]. The purpose of the GDL is realized by effectively distributing the reactant gases into the CL for the electrochemical reaction, while simultaneously allowing electron and water transport from the CL to the current collector [44]. Therefore, the GDL has to be rationally designed to facilitate reactant gas diffusion and product water removal. The use of a graded GDL with gradients of porosity and hydrophobicity are the two main optimization strategies.

## 3.1 Graded Distribution of Porosity

When more void space within the GDL is occupied by carbon materials, the porosity of the GDL is reduced, and vice versa. It is expected that a decrease in the GDL porosity leads to a higher effective electronic conductivity of the GDL. Unfortunately, this may hinder the transport of reactant gases in the GDL. In particular, when using air as the cathode reactant gas, the dilution effect of nitrogen causes extra oxygen transport limitation at the cathode [45]. In contrast, an increase in the GDL porosity facilitates the gas supply but reduces the electron conduction. In addition, the GDL porosity significantly affects the distributions of reactant gases and current density over the CL. Therefore, the development of a porosity-gradient GDL to achieve a moderate increase in the gas transport rate without severely decreasing the electronic conductivity is an approach worthy of consideration.

Along the through-plane direction, Chu et al. [46] numerically studied the effects of various GDL porosities on the performance of fuel cells with nonuniform GDL porosity by using a half-cell model. The oxygen mass fraction distribution in the channel and porous electrodes, the membrane phase potential, and the predicted current density were investigated. The results revealed that GDL porosity had a limited or negligible influence on the level of polarization at low and medium current densities but exerted a significant influence at high current densities. This conclusion was confirmed by the numerical and experimental results of Roshandel et al. [47], although the effects of the phase change and liquid water in their model were omitted. Chen [48] employed a multiphase mixture model to study the GDL porosity gradient formed by adding microporous layers (MPLs) with different carbon loadings on the CL side and on the flow field side, respectively. The model assessed the water saturation and oxygen concentration across the GDL, as well as the resulting activation and concentration losses. The results showed that a gradient of porosity benefited the removal rate of liquid water and enhanced the transport of oxygen through the cathode GDL, thereby leading to improvement of the cell performance. Huang et al. [49] developed a three-dimensional, two-phase, nonisothermal model to explore the enhancement of water transport by a linear porosity gradient in the cathode GDL. The simulation results suggested remarkable improvement of the limiting current density and oxygen usage with an optimal linear porosity gradient with a porosity of 70% near the channel and 30% near the CL for the parallel and z-serpentine channel designs, as shown in Fig. 4. It was found that the current density increases from 1.41 to 1.66 A $cm^{-2}$ when the abovementioned graded porosity distribution was applied. The same trends are also observed for parallel and interdigitated channel designs. Zhan et al. [50, 51] developed a one-dimensional model to study the distribution of liquid water saturation for GDLs structured with a gradient porosity distribution. According to the computational outcomes, with the same average equivalent porosity, a larger porosity gradient leads to easier gas diffusion. A GDL with a gradient of porosity was preferable for liquid water discharge from the electrodes into the flow channels. The optimization of the GDL gradient structure showed that a GDL with a linear porosity distribution was the best for cell performance.

Along the in-plane direction, Sinha et al. [52] investigated tortuosity-graded gas diffusion media with fine and coarse structures along the cathode flow channel, respectively. As shown in Fig. 5, the coarse section provided faster oxygen transport and improved cell performance toward the outlet due to its low tortuosity, while the fine section offered better water retention due to its high tortuosity. Therefore, proper selection of the lengths of the fine and coarse sections was vitally important to improving cell performance. Recently, Zhang et al. [53] explored the porosity-graded GDLs, in which the GDL porosity exponentially increased along the flow channel from the inlet to the outlet. In their work, both a mathematic model and an optimization algorithm were used to numerically investigate the optimal distribution of the GDL porosity along the flow channel. Experiments were also conducted to measure the local current density distribution and evaluate the effects of the graded porosity distribution in the GDLs. It was concluded that using an optimally graded porosity distribution improved the current density uniformity and maximized the cell power density.

Kimball et al. [54] suggested that the generated liquid water enters the largest pores of the GDL, and considerable pores of the GDL remain free of liquid water due to their hydrophobicity. The water flows from the membrane/electrode interface to the gas flow channel, detaches as water drops and then forms liquid slugs along the air flow within the cathode flow channel. Since the void space of the GDL was prone to being blocked near the outlet of the channel due to the build-up of water slugs, the designed porosity in the region needs to be extremely high to enhance oxygen transport. A higher GDL porosity near the gas flow channel and a lower GDL porosity near the CL improved the performance of the fuel cell at high current densities. The decrease in porosity increases the capillary force, squeezing liquid water into the more porous region; thus, the rational control of the GDL gradient enhances the liquid water removal.

## 3.2 Graded Distribution of Hydrophobicity

The graded hydrophobic GDL is achieved by designing a graded distribution of polytetrafluoroethylene (PTFE) inside the GDL. The increase in the amount of PTFE, on one hand, remarkably improves the hydrophobicity of the GDL, and on the other hand, lowers the reactant gas diffusivity through the reduced-size pores. In addition, increasing the PTFE loadings also hampers the liquid water removal due to the reduced pore size and volume, and it simultaneously decreases the electrical resistance [55]. It is thus reasonable to optimize the amount of PTFE in the GDL to tradeoff the positive and negative impacts.

The profiles of the PTFE distribution within the porous electrodes were mainly determined by the drying conditions. Due to the difficulty in PTFE penetrating through the electrodes, a heterogeneous distribution along the through-plane direction was generated as a result of typical spray/brush technologies and drying at atmospheric pressure [56]. Because the typical GDL pore size is approximately 10-30 μm, PTFE particles between 50 to 500 nm could penetrate through the GDL easily [57]. Mathias et al. [58] experimentally measured the PTFE distribution along the through-plane direction with a variety of drying times. It was found that a high PTFE concentration region moved from the GDL surface to the interior when a longer drying time was applied, which was likely due to the influence of gravity. Kang et al. [59] investigated the water profiles within the GDL using the two-phase fuel cell model and found that the maximum water content was located near the center of the GDL. The GDL wettability in the through-plane direction was assumed to be initiated by the spatial variation of PTFE within the GDL. Due to the incomplete PTFE treatment inside the interior GDL, the pores in this area are more hydrophilic, which could lead to easier accumulation of water. In other words, less PTFE-coated pores were prepared in the inner GDL, as shown in Fig. 6. In this figure, we can see the SEM images and corresponding EDS maps for F over the cross-sectional area of the GDL prepared by an air-dried PTFE strategy. One can clearly see the heterogeneous distribution of PTFE, with higher loadings near both the upper and lower surfaces of the GDL. To solve this problem, Ito et al. [60-62] increased the PTFE content inside the Ti-felt GDL (a type of GDL made from 20 μm-diameter titanium fibers) and drying under

vacuum pressure. The novel methods in this work improved the current density by approximately 1.9 times at 0.6 V in comparison with the case of a nonuniform PTFE distribution. The effect of the PEFE distribution in the GDL was important even when an MPL was included. The capillary diffusion coefficient is proportional to the contact angle of the water droplet on the substrate surface [63, 64]. A higher capillary diffusion coefficient in the GDL near the membrane than that near the gas flow channel is capable of pushing liquid water to the channel at a faster rate. Thus, it is believed that placing more PTFE near the membrane is a strategy for enhancing the cell performance at high current densities and high relative humidity.

There are few studies available for the in-plane PTFE distribution in the GDLs. The effects of the inhomogeneous distribution of PTFE along the in-plane direction have been seldom investigated. An experimental study of the in-plane PTFE gradients inside GDLs was carried out by Vijay et al. [65], wherein PTFE gradients along the in-plane direction were obtained by exploiting capillary wicking of the PTFE suspension. More effective water management was achieved from the in-plane distribution of PTFE. Theoretically, along the in-plane direction, the PTFE content near the outlet should be higher because water is prone to accumulate in this region. At low reactant gas stoichiometric flow ratios, capillary diffusion is the primary driving force for liquid water expulsion through porous electrodes [66]. The shear forces play a more important role in liquid water expulsion with high reactant gas stoichiometry [67]. The shear force can be related to the contact angle, which is directly affected by the PTFE content. Due to the variation in contact angles along the in-plane direction, various water removal capabilities along the reactant flow direction are expected. A higher water expulsion rate near the outlet can be utilized to counteract water flooding in this region. The graded designs of porosity and hydrophobicity of the GDL were summarized in Table 1.

# 4. Graded MPL

An MPL is typically made of carbon black powder, hydrophobic PTFE and binder materials, such as ink (a multicomponent suspension of carbon powder, binder and PTFE et al.) for this application. The

thickness of an MPL is typically tens of micrometers. In achieving better cell performance at medium and high current densities, the MPL plays a critical role, particularly when the effect of water flooding becomes significant. The role of the MPL is to properly manage reactant gas transport and water discharge. It is suggested that a compact, thin MPL with high hydrophobicity could significantly decrease the liquid water saturation inside the CL [68-73]. According to the mass transport mechanism in the microstructure of an MPL, the rational design of the distributions of porosity and hydrophobicity within the MPL is important in enhancing the cell performance.

A multilayer MPL is practically used for fuel cell applications because it increases the limiting current density in terms of reducing the ohmic overpotential and reinforcing mass transport due to the improved ionic conductivity and water removal rate [68]. A multilayer MPL is more suitable for PEM fuel cells with higher power applications under extremely wet operating conditions, while a single MPL is typically sufficient for low-power cells with low levels of water flooding.

## 4.1 Graded Distribution of Porosity

The function of the MPL is similar to that of the GDL [69], with the best difference being the smaller pore size of the MPL. For this reason, the pore distribution inside the MPL more significantly affects the transport of reactant gases and produced water, which then affects the apparent cell performance. Specifically, the liquid water inside the MPL near the GDL side is significantly decreased to avoid flooding. Meanwhile, water inside the MPL near the CL side is well-maintained to provide a good membrane hydration condition. To prepare the porosity-graded MPL, introducing a pore-forming agent such as ammonium chloride ($NH_4Cl$) or thermally expandable materials such as graphite are strategies commonly used [70, 71]. For efficient gas and liquid water transport inside the GDL, different pores of various sizes in the micro, meso and macro ranges are required. A large number of hydrophobic meso-pores are needed for reactant gas diffusion to catalytic sites via micropores. Moreover, more hydrophobic macropores are essential for liquid water removal under a certain capillary pressure. Therefore, the pore

size inside the MPL near the MPL/GDL interface should be larger than that near the CL/MPL interface for effective water removal to the channel.

Wang et al. [72] prepared MPLs from different carbon materials, namely, 80 wt% acetylene black carbon and 20 wt% Black Pearls 2000 carbon, to enhance the transportation of both reactant gases and liquid water. Furthermore, a novel graded-porosity GDL was proposed by adding MPLs with different carbon loadings to the CL side and to the flow field side for improved liquid water removal. By the rational adjustment of the pore size distribution and wettability, they found that an MPL with a gradient configuration of 0.7/0.3 (ratio of carbon loading in the MPL at the CL side to that at the flow field side) with carbon loadings of 0.7 mg $cm^{-2}$ on the CL side and 0.3 mg $cm^{-2}$ on the flow filed side is preferable for improved cell performance.

Chun et al. [70] prepared a porosity-graded MPL using the double coating method to enhance the water removal ability of the GDL. Thermal expandable graphite (TEG) was applied to control the porosity of each layer. The porosity gradually increased from the MPL/CL interface to the gas diffusion backing layer (GDBL)/MPL interface. The comparison of cell performance obtained from the porosity-graded MPL and conventional MPL showed improved water permeability and cell performance at high current densities. In the work of Tang et al. [71], the MPL was prepared by printing different contents of $NH_4Cl$ pore-former, and the porosity of the MPL decreased from the inner layer at the CL/MPL interface to the outer layer at the GDL/MPL interface. The cell consisting of a porosity-graded MPL has better performance than that consisting of a homogeneous MPL, especially at high current densities. The reason is the increased capillary force of the graded porosity in MPL, which hence increases the water expelling capacity of the electrode.

Previous results from different researchers showed a different optimal distribution of porosity inside the MPL. This may be explained by the various pore sizes obtained through different methods. For example, the pore diameter ranged from approximately 620 to 1020 nm, with a mean value of 733.1 nm, in Chun's report [70]. In contrast, the pore size distribution was between 0.01 and 10 μm in Tang's work

[71]. As stated, there were two main types of pores, with the pore sizes between 10 and 80 nm and between 80 nm and 10 μm, and the pore volume of the later type exceeds that of the former type. The MPL pore size obtained by Tang et al. is much larger than that by Chun et al. In this case, the optimal porosity distribution can be a gradual decrease from the CL/MPL interface to the MPL/GDL interface. In spite of the low porosity near the MPL/GDL interface, the liquid water discharge and gas transport are not significantly affected due to the large pore size in this region. In the case of a very small pore size, the low porosity near the MPL/GDL interface would cause pronounced mass transport resistance in liquid water expulsion to the gas flow channel, resulting in flooding inside the porous electrode.

## 4.2 Graded Distribution of Hydrophobicity

Similar to the PTFE distribution of GDLs, the optimal distribution of PTFE within the MPL obeys a decreasing gradient from the CL/MPL interface to the MPL/GDL interface. Weng et al. [73] designed a hydrophobicity-graded MPL and experimentally studied the cell performance under a variety of humidification conditions. Three MPLs with various PTFE contents, 20, 25 and 30 wt% in the MPLs from the CL/MPL interface to the MPL/GDL interface, were sandwiched between the CL and GDL. Thanks to the relatively low PTFE loading inside the inner layer of the as-prepared MPL, product water from the oxygen reduction reaction was retained within the CL under low humidity conditions, e.g., 5%. In contrast, the hydrophobicity-graded MPL efficiently discharged liquid water from the porous electrodes at high relative humidity, e.g., 50%, leading to improved cell performance, as shown in Fig. 7. The increase in PTFE loading near the membrane alters the permeability of water transport through the GDL. In the GMPL, the decreasing permeability from the membrane to the GDL helps maintain water inside the MEA, leading to improved cell performance at low relative humidity. Note that too much PTFE near the MPL/GDL interface, e.g., 35 wt%, would block pores for water removal through the GDLs, leading to water flooding within the CLs and, eventually, a drop in cell performance at high relative

humidity. Thus, the optimal gradient of the PTFE content in the MPL has to be precisely controlled. The graded designs of porosity and hydrophobicity of the MPL were summarized in Table 2.

# 5. Graded CL

The CL is one of the most complicated parts of the whole MEA. It consists of necessary components for electrochemical reactions and proton and charge transfer, as well as void space for reactant gas transport and liquid water discharge. Due to the highly compacted structure required within a limited thickness (typically several micrometers), experimental investigations are difficult, expensive and sometimes not feasible. Instead, a numerical study could provide detailed information for guiding the CL design. Prior to the numerical design of a graded CL, the development of proper models to represent the morphology of the CL is essential. Numerous models were chronologically developed to study the influence of the CL on the cell performance, for example, ultrathin or interface layers [74, 75] and microhomogeneous [76-78] and agglomerate [79, 80] models. Among these models, interface and microhomogeneous models can hardly match the cell behavior under a large range of operating conditions due to the great difference between computational geometries and practical CL structures. Sun et al. [81] developed an improved two-dimensional, spherical agglomerate model for the cathode of a PEM fuel cell. This model assumed that platinum particles were embedded into the spherical carbon agglomerates, which were cross-linked by the ionomer polymer network. They showed that both proton and electron transport played important roles in determining the electrochemical reaction rate and local cathode overpotential. The extra mass transport resistance to oxygen transport, initiated by ionomer films surrounding the agglomerates, was significantly important in high-current density cell operation. Recently, Cetinbas [80, 82] et al. improved the classic agglomerate model by representing the catalyst as a discrete platinum particle distribution. The influence of a random platinum particle distribution within the agglomerate was investigated and the diffusion-limited region at various catalyst loadings was investigated. Based on the agglomerate model, a typical form of the volumetric current density can be written as follows [81, 83-85]:

$$i_{agg,i} = n_i F \left(\frac{p_i}{c_i^{ref} H_i}\right)^{\gamma} \left[ \frac{1}{E_{agg,i} k_{agg,i}} + \frac{r_{agg} + \delta_M + \delta_{w,i}}{r_{agg}} \left( \frac{\delta_M}{a_{agg,i}^M D_{i-M}} + \frac{\delta_{w,i}}{a_{agg,i}^w D_{i-w}} \right) \right] \quad (5)$$

with

$$k_{agg,i} = \frac{a_{agg,i}^M i_{0,i}^{ref}}{n_i F} \left[ \exp\left(\frac{-\alpha_{Rd,i} F \eta_i}{RT}\right) - \exp\left(\frac{\alpha_{Ox,i} F \eta_i}{RT}\right) \right] \quad (6)$$

where the subscript $i$ represents the anode and cathode and the superscript $\gamma$ equals 0.5 for the hydrogen oxidation reaction (HOR) at the anode and 1.0 for the ORR at the cathode, respectively. $p_i$ (Pa) and $k_{agg,i}$ ($s^{-1}$) are the partial pressure and the reaction rate coefficient of species $i$. $E_{agg,i}$ and $\delta_{w,i}$ (m) are the effectiveness factor and liquid water film thickness at the anode and cathode, respectively. $a_{agg,i}^M$ ($m^{-1}$) is the active electrochemical surface area available for the reaction. $\alpha_{Rd,i}$ and $\alpha_{Ox,i}$ are the reduction and oxidation reaction charge transfer coefficients, respectively.

If the electrode is considered as an isotropic media, the effective electronic conductivity is normally obtained from the Bruggeman correction due to the very large intrinsic electronic conductivity of carbon materials in comparison with the proton conductivity of polymers as follows [86, 87]:

$$\sigma_s^{eff} = \sigma_s (1 - \varepsilon_{CL})^{1.5} \quad (7)$$

To consider the effect of the contact area between agglomerates, the effective proton conductivity is estimated by the following equation [83]:

$$\sigma_M^{eff} = (1 - \varepsilon_{CL}) \left[ 1 + \frac{(\%M \varepsilon_{CL} - 1)}{(1 + \delta_M / r_{agg} + a_0)^3} \right] \sigma_M \quad (8)$$

where $\sigma_s^{eff}$ and $\sigma_M^{eff}$ (S $m^{-1}$) are the effective electronic and proton conductivities of the CL, respectively. $\%M$ is the primary pore volume fraction occupied by the ionomer, and $\varepsilon_{CL}$ is the catalyst layer porosity.

The intrinsic conductivity of the Nafion membrane is a function of temperature (T) in Kelvin and the membrane water content ($\lambda$), as expressed in the following equation [88, 89]:

$$\sigma_M = \exp[1268(\frac{1}{303} - \frac{1}{T})](0.5139\lambda - 0.326) \quad (9)$$

Eqns. (5) - (6) are used to describe the electrochemical kinetics while Eqns. (7) - (9) are adapted for the effective electronic and ionic conductivities. These equations, obtained from literatures, have been commonly used in PEM fuel cell models.

## 5.1 Graded Distribution of the Nafion Ionomer

The Nafion ionomer typically occupies the large pores of the CL and builds up a cross-linked network of ionomer matrix for proton transport [90, 91]. A higher ionomer content is, on one hand, beneficial to the ionic conductivity; however, on the other hand, it blocks the void space inside the CL and increases the mass transport resistance of gas diffusion and water removal. An optimal Nafion content yields a minimal species transport resistance while maintaining good conductivity of the CL. The graded CL with a higher content of ionomer near the membrane and a low content of ionomer near the GDL is considered a novel design for the improvement of cell performance at medium and large current densities.

Numerous previous studies proved that reducing the Nafion content from the region near the membrane toward the GDL, along a certain gradient, is capable of improving the cell performance, especially at high current densities. Wang et al. [92] developed a macrohomogeneous model to explore the systematic effect of the Nafion content on the cell performance. It revealed that a Nafion content of approximately 35 wt% was capable of balancing the gas and ion transport, as well as providing an electrochemically active surface area for the ORR. Thus, the best cell performance was achieved with this Nafion loading. In their following experimental study [93], as shown in Fig. 8, the uniform and graded porous electrodes were compared at different operating temperatures, with the uniform electrode containing 30 wt% Nafion and the graded electrode being integrated with three sublayers containing various Nafion contents from 20 wt%

to 40 wt%. The results indicated that at intermediate and high current densities, placing more Nafion near the CL/membrane boundary and less Nafion near the CL/GDL interface could improve the cathodic performance of the cell. In contrast, cell performance significantly declined when the gradient of Nafion content was reversed. This can be explained by the increase in ionic conductivity affecting proton transport near the interface of catalyst layer and membrane (CL/membrane) and by the increase in electrode porosity affecting gas transport near the interface of the catalyst layer and gas-diffusion layer (CL/GDL), respectively. Kim et al. [94] prepared MEAs that had two different compositions of CLs in the electrodes, with the one close to the membrane (inner layer) having a higher Nafion content and the other near the gas diffusion layer (outer layer) having a lower Nafion content. It was found that 33 wt% and 23 wt% are the optimal Nafion ionomer contents of the inner and outer layers, respectively, for maximum cell performance at current densities higher than 800 mA $cm^{-2}$.

A graded distribution of platinum loading and the platinum-to-carbon ratio (%*Pt/C*) are typically considered in optimizing the Nafion content in the graded electrode design. Su et al. [95] prepared a novel double CL (NDCL) cathode with various Pt and Nafion contents inside the inner and outer CLs with different thicknesses. The morphology and cell performance of different MEAs were compared with those of a single CL (SCL), traditional double CL (DCL) and NDCL, as shown in Fig. 9. In the cross-sectional SEM images, the upper CLs belong to the anode, while the lower CLs are on the cathode side. One can see that the CL thicknesses are roughly the same with respect to the different preparation methods. The cell performances of four DCL cathodes were then measured and compared with that of the SCL cathode. They concluded that superior cell performance was achieved when the Pt ratio and Nafion contents within the inner and outer CLs were controlled at 8:2 and 33 wt % and 20 wt %, respectively. The new DCL cathode resulted in an increase in current density by 35.9% at 0.6 V in comparison with that in the traditional electrode. This enhancement is primarily attributable to the increase in porosity of the outer layer with low Pt and Nafion contents, which is of benefit to oxygen mass transport and liquid water removal. Song et al. [96] numerically performed both single-variable and two-variable optimization of the platinum loading and Nafion content. It was demonstrated that linear increases of both the Nafion content

and Pt loading from the interface of the GDL/CL to that of the CL/membrane were the optimal functions of Pt loading and the Nafion content when they were separately studied as single variables. However, when a two-variable optimization algorithm was performed, the optimal distribution of the Nafion content still followed a linearly increasing function, but the optimal distribution of Pt loading followed a convex increasing function. Briefly, higher contents of both platinum and Nafion near the CL/membrane interface were desirable for improved cell performance. However, a rational design of Nafion profiles within the CL was much more important than that of platinum.

To the best knowledge of the authors, there are only few studies that have examined the effect of the in-plane distribution of Nafion on the cell performance. Because the Nafion content/distribution-related proton and water transport seems more important along the through-plane direction than along the in-plane direction, Cetinbas et al. [97] numerically studied bidirectionally graded CL compositions and the effects of catalyst and ionomer loadings in both the through-plane and in-plane directions. Their study elucidated that a higher Nafion weigh ratio under the channel, in comparison with that under land, enhanced the cell performance due to the improved ion transport. Recently, Herden et al. [98] manufactured a segmented cathode with various ionomer equivalent weights within the upstream and downstream regions of reactant gases. It was found that the cell performance was improved by the in-plane distribution of ionomer equivalent weights under a wide range of operating conditions. The electrode with a lower equivalent weight near the inlet and a higher equivalent weight near the outlet showed better performance than did the homogeneous electrode.

## 5.2 Graded Distribution of Platinum Catalysts

For Pt-based CLs, the platinum particles must be well-dispersed and rationally distributed inside the CL to guarantee a high specific area and catalytic activity. When fuel cells operate under a variety of loads, the required activities and mass transport rates are varied owing to the nonuniform spatial distribution of reactant gases and the volume change of the void space initiated by the formation of liquid water.

Therefore, rational manipulation of the spatial distribution of platinum within the CL is helpful in reducing the amount and improving the efficiency of the precious catalyst.

The concentration of reactant gases decreases and the amount of water increases from the GDL to the PEM as the reactants are consumed and products are formed. In particular, the kinetics of the ORR at the cathode are much slower than those of the HOR at the anode. Therefore, for the relatively sluggish ORR at the cathode, the oxygen diffusivity decreases due to the higher liquid-water flooding within the porous electrode; therefore, the rate of the ORR is further deteriorated. Thus, the design of a through-plane graded Pt distribution is considered a promising strategy for reducing the Pt usage without decreasing the cell performance. Most experiments have applied a multilayer design to study the optimal platinum gradient for a novel CL. Antoine et al. [99] studied the effects of catalyst loading gradients on cell performance with two types of electrodes, nonporous and porous. For the former type of electrode, more catalysts near the CL/GDL interface maximized the cell performance, but for the latter type of electrode, a higher concentration of catalyst near the CL/membrane interface is an optimal strategy. Taylor et al. [100] utilized an inkjet printing (IJP) method to prepare a graded catalyst structure with the highest platinum concentration in the region closest to the PEM and the lowest concentration furthest away. The preparation of such a graded CL using this method achieves improved cell performance in comparison with that of the traditional CL. Matsuda et al. [101] experimentally studied the effect of a multilayered CL design on cell performance. The activities of the reaction areas near the GDL and membrane under various relative humidity conditions were particularly investigated. Their results suggested a variation of catalyst loadings within the CL at different relative humidity values. When the relative humidity increased, the partial pressure of oxygen decreased. Under this condition, the catalyst loading should be higher near the GDL side to oxidize the oxygen more efficiently. For fuel cells using polybenzimidazole (PBI) as membrane, Kongstein et al. [102] constructed a DCL with 50 wt% Pt/C close to the membrane and 20 wt% Pt/C farther away. A maximum power density of 0.83 W $cm^{-2}$ at 0.4 V was achieved using the as-prepared MEA. Su et al. [103] experimentally investigated the content and distribution of platinum in a DCL based on using polytetrafluoroethylene (PTFE) and polyvinylidene difluoride (PVDF) as two

types of binders. They found that a high Pt content in the PVDF CL benefited the electrode kinetics, while a high Pt content in the PTFE CL favored the mass transport. In their experiment, PTFE- and PVDF-based CLs were respectively used as inner and outer layers of the MEA. Proper Pt distributions in the DCL, e.g., a Pt mass ratio of 3:7 in the inner and outer layers, resulted in improved single-cell performance and durability.

Roshandel and Ahmadi [104] numerically studied the spatial variation of catalyst loading in two directions based on the agglomerate assumption. It was found that the key question of where to apply more catalyst to increase the power density is addressed by the identification of locations at which the reaction occurs at the highest rate. The CL porosity was assumed to be 20%, and liquid water formation was ignored in this model. In this case, applying more catalyst under the channel and near the CL/membrane interface yielded improved cell performance. Taking the impact of liquid water formation and transport into account, Srinivasarao et al. [105] developed a two-dimensional and two-phase model to optimize the platinum loading, ionomer loading, weight fraction of platinum on carbon, and CL thickness of a novel design with multiple CLs. They suggested that to achieve the same cell performance as that obtained from a single CL design, the overall loading of platinum should be reduced when a multilayer CL is applied. Moreover, the optimal platinum loading of the CL close to the GDL was higher than that of the CL close to the membrane, as shown in Fig. 10. In this figure, CL1 represents the MPL-CL interface and CL4 corresponds to the CL-membrane interface. In the base case design, the platinum loading was fixed at 0.25 mg $cm^{-2}$ and uniformly distributed in different sublayers. At high cell voltages, the optimal platinum distribution almost does not change. At decreasing cell voltage, which corresponds to an increase in current density, the optimal platinum loading decreases from the CL-membrane interface toward the MPL-CL interface. At 0.4 V, the optimal platinum loading within the CL-membrane interface decreases to 0.15 mg $cm^{-2}$. This trend was confirmed by the work of Xing et al. [106]. The novel multilayer CLs with a graded platinum loading design improved the current density by approximately 15% at high current densities and by approximately 85% at low current densities.

The majority of experimental studies indicated that more platinum loading near the membrane could improve the cell performance [99-101]. However, such improvement was more significant in fuel cells operated at low and medium current densities. This is because at high current densities, the formation of considerable amounts of liquid water was very likely to block the void space for gas transport inside the porous electrode, leading to low utilization of the catalyst near the membrane. Other numerical studies showed different results, wherein more platinum loading near the GDL rather than near the membrane improved the cell performance [105, 106]. This can be explained by the assumptions in most numerical models, with the catalyst particles assumed interact well with the ionomer based on the continuum mechanics. In other words, all catalyst particles were used to form the triple phase boundaries (TPBs) on the surface of the continuous ionomer network. Once the two-phase flow between gas and water was taken into account, the higher platinum loading near the GDL was good for the cell performance, especially at high current densities. Due to the limitations of experimental fabrication, the catalyst particles near the membrane were more likely to be connected to ionomers, whereas those away from the membrane may have had a lower chance to build up the TPBs. Theoretically, placing more platinum near the GDL is capable of increasing the possibility of platinum particles being exposed to higher concentrations of reactant gases. Moreover, the reactant gas concentration decreases along the through-plane direction from the GDL/CL interface toward the CL/membrane interface. Therefore, a higher CL porosity near the GDL/CL interface is an optimal design to guarantee a relatively high volume of available reactant gases [98].

Due to the accumulation of liquid water and heat along the gas flow direction, the CLs near the outlet of the electrode become hotter and less porous, leading to nonuniform performance over the active electrode area. Under these conditions, the inhomogeneous current density distribution inside the catalyst layer would accelerate the degradation of the electrode. To mitigate this problem, the graded distribution of platinum along the in-plane direction is considered as a possible solution. As shown in Fig. 11, Santis et al. [107] designed a tailored cathode with redistributed along-the-channel catalyst loading, with the loading lower near the inlet and higher near the outlet of the cathode. The average platinum loading is

between 0.25 and 0.3 mg $cm^{-2}$. Cases of higher platinum loading near the inlet and lower loading near the inlet were also compared. For the same average platinum loading of 0.3 mg $cm^{-2}$, an increase in platinum loading along the gas flow direction improved the cell performance by 20% at 0.5 V. It has also been indicated by both experimental and numerical results that the optimal gradient of catalyst loading depends on the air stoichiometry. A gentle increase of the catalyst loading profile homogenized the current density at relatively higher air stoichiometries, while a steeper profile was better suited for lower air stoichiometries. To improve catalyst utilization and reduce platinum usage without remarkable loss in cell performance, Prasanna et al. [108] increased the local electrochemical reaction rate by applying a catalyst-gradient electrode method to single-cell fabrication. In this work, more catalysts were placed near the outlet of the cathode channel, so that the depletion of oxygen along the channel was counteracted by the increased catalyst loading. With the help of the catalyst-gradient electrode, the cell voltage increased from 0.56 to 0.61 V at a current density of 0.9 A $cm^{-2}$, and the peak power density increased from 0.5 to 0.59 W $cm^{-2}$ with a platinum loading of 0.3 mg $cm^{-2}$. Recently, Xing et al. [109] found a strong interaction between the platinum loading and GDL porosity through the developed two-phase flow CFD model and experimental validation. The improvement of cell performance by placing more Pt near the outlet region at the cathode was recommended. However, homogenization of the current density also strongly depends on the graded GDL porosity. To achieve a homogeneous current density along the flow channel, the critical issue is to spatially match the electrochemical and species transport rates. When a high platinum loading and GDL porosity are initially applied at the cathode inlet, the individual increment of platinum loading near the outlet cannot improve the cell performance and current density uniformity. A systematic design of the gradients of platinum loading and GDL porosity must be taken into account.

Successful operation of a fuel cell typically requires the supply of humidified reactant gases through an auxiliary humidifier. The associated increase in volume and weight results in a challenge in the commercialization of PEM fuel cells as portable energy sources. One of the possible ways to mitigate this challenge is to modify the fuel cells for operation without external humidification. For fuel cells using a

self-humidifying membrane as the electrolyte, a catalyst-gradient electrode is also an important alternative. Lee et al. [110] designed a novel electrode by introducing the catalyst gradient coating method for the MEA. To hydrate the PEM using the self-produced water, more ORR catalysts were located near the cathode inlet, and catalyst loading gradually decreased toward the cathode outlet. An improvement of cell performance by approximately 17% under nonhumidified conditions resulted from the catalyst-graded design in comparison with the conventional design. Penga et al. [111] manufactured a variable-temperature flow field for PEM fuel cells, which allowed maintaining nearly 100% relative humidity along the entire flow field without external humidification. A five-segment cell with graded operating temperatures was implemented in their work. It was found that a higher temperature at the segment closer to the outlet retains more moisture generated by the ORR. The novel design reduced mass transport losses at the high current density range by minimizing the water flooding within the cell.

The graded design of porosity within the CL is a big challenge due to the very limited thickness of the component; therefore, available publications on this subject are very limited. Nevertheless, the variation in platinum loading and ionomer loading inevitably change the CL porosity. It is believed that the influence of the graded porosity is included in the effects of graded designs of platinum and ionomers. Wang et al. [112] designed a dual-porosity Pt/C as the ORR catalyst, in which ordered macro- and mesopores were arranged. The novel catalyst showed significantly improved anti-flooding ability and durability. The graded designs of platinum and ionomer loadings of the CL were summarized in Table 3.

# 6. Graded PEM

For a function-graded PEM, a gradient density of sulfonic acid groups along the membrane thickness direction is typically used as the definition [113]. In most previous studies, such partially fluorinated sulfonic acid membranes (part-FSAs) were prepared using irradiation methods, e.g., a low-energy electron beam (EB) [114, 115]. The mechanism of improving the cell performance is the control of the membrane water uptake.

Sato et al. [113] fabricated an FN (hybrid membrane) by mixing s-FEP (sulfonated radiation-grafted membrane) powder with a Nafion dispersion and compared the water uptake, ion exchange capacity (IEC) and cell performance achieved by using FN, s-FEP and Nafion®112 as the membrane, respectively. The IEC and water uptake of the FN was improved compared to those of the Nafion112 and s-FEP, resulting in the highest cell performance among the tested membranes, as shown in Fig. 12. Fujita et al. [114, 115] fabricated a novel PEM with functionally graded sulfonated acid groups utilizing the low-energy EB grafting method. The sulfonated acid groups were rich on the anode side and poor on the cathode side in the as-prepared new PEM. The cell performance was significantly improved in the high current density range, which was attributed to the gradient of water uptake. The higher membrane water content at the anode side prevented dehydration of the membrane at the anode and mitigated water flooding at the cathode side. The gradient-PEM therefore offered a promising solution for better water management in MEA. Shirarki et al. [116] changed the properties of polymeric materials and synthesized a novel PEM with variation of the sulfonic acid group density using the $Xe^{54+}$ heavy-ion beam with the energy of 6 MeV/u under vacuum conditions. It was shown that the MEA with functionally graded PEM improved the performance of the fuel cell. It was considered that the functionally graded PEM could control the water behavior due to the graded distribution of sulfonic acid. Tsuchida et al. [117] compared the functionally graded PEMs (G-PEMs) with Nafion 212 and normal PEMs (N-PEMs) under nonhumidified conditions. Due to the difference in proton transfer kinetics among different PEMs, the as-prepared G-PEMs showed better performance and durability than did commercial Nafion 212 and N-PEMs at the two temperatures. The best cell performance was obtained using the decreasing-type G-PEMs, representing a decrease in ionic sites from the anode to the cathode side in the PEM, which can be explained by the prevention of drying due to the higher ion exchange capacities (IECs) and back diffusion.

The above experimental work was supported by the theoretical outcomes of Verma and Pitchumani [118]. They presented a dynamic model for a single-channel PEM fuel cell for understanding the effects of membrane properties on the transient behavior of water transport, wherein the cell performance is

critically related to the water content of the membrane. It was shown that a sudden increase in the current density can lead to anode drying, which causes voltage reversal and may lead to cell degradation. It was also suggested that a graded membrane design with a decreasing water content across the membrane thickness from the anode to the cathode was a possible approach to prevent anode dehydration and avoid irreversible damage to the membrane. The graded design of sulfonic acid group of the PEM was summarized in Table 4.

# 7. Multi-Variable Optimization

Referring to the graded design of the functional components involved inside the MEA of a PEM fuel cell, changing the distributions of multiple components typically results in improved cell performance in comparison with that from changing a single-component [95, 98, 105]. However, optimization of the porous electrodes and PEM of a fuel cell is a challenging task because a multitude of design parameters must be optimized simultaneously to attain the optimal cell performance. The number of possible designs increases sharply as the number of design variables increases. Since the optimal graded distributions of different components are simultaneously preceded in parallel, e.g., the design of both a graded GDL and a graded MPL [119], multivariable optimization is an efficient method by which to optimize the cell performance by simultaneously optimizing a variety of variables. The common principle of numerical optimization is to efficiently search for an optimal design in a coupled mathematical algorithm with the aid of a computational analysis tool. Only a few designs need to be evaluated using the optimization algorithm, and the computational time is therefore significantly reduced. The multivariable optimization helps researchers create new designs or improve existing ones. Song et al. [120, 121] are considered the pioneers of the optimization of cell electrodes using a numerical optimization approach. The CL composition, including the ionomer volume fraction, catalyst layer thickness and catalyst loading, was optimized to achieve the maximum current density at the cell voltage of 0.6 V. The optimal distributions of Nafion ionomers and platinum were obtained. The optimization results indicated that the optimal

ionomer loading was approximately 30 wt. % [120], and the cell performance was improved by placing more ionomer and platinum near the membrane [121].

Secanell et al. optimized both the platinum loading and performance of a complete MEA [122, 123] based on their optimization framework developed previously [124]. The design variables included the platinum loading, ionomer loading, GDL porosity and platinum mass ratio. It is shown that the cell performance was significantly improved by using the parameters obtained from the optimal design. The optimization results suggested that the cell performance can be improved by increasing the ionomer content and reducing the catalyst loadings. In addition, the platinum loading had to be controlled within the range of 0.1 to 0.5 mg $cm^{-2}$, as higher loadings resulted in the waste of platinum rather than an increase in current density. Srinivasarao et al. [105] investigated an innovative design of a PEM fuel cell with multiple CLs. The design variables, including the weight fraction of platinum relative to carbon, platinum loading, ionomer loading, and thicknesses of all the CLs, were optimized to satisfy two objective functions. One objective was to maximize the current density at a specific cell voltage, while the other objective was to minimize the platinum loading for a given current density. A two-objective function multivariable optimization of the cathode composition of the PEM fuel cell was carried out by Xing et al. [125]. Five design variables, including the platinum loading, Pt/C ratio, ionomer volume fraction, thickness of the CL and agglomerate size, were optimized through a multiple surrogate model, and their sensitivities were analyzed by a Monte Carlo method-based approach. As a novel optimization strategy, maximizing the current density within a specific range of cell voltages was implemented for prediction of the optimum values.

Numerical optimization is able to provide insight for porous electrode designs including cost reduction, performance improvement, and efficiency increase. As a relatively new research area, the numerical optimization of fuel cells has attracted growing interest.

# 8. Conclusion

The functionally graded design of the MEA, including the GDL, CL, MPL and membrane, has been reviewed in terms of experimental studies and numerical analysis. The graded design affects the mass transport of water and gases, electrode activity, heat transfer, electronic and ionic conductivity, and, consequently, the potential and current distributions and the cell voltage and power generated under different operating conditions. Owning to the spatial orientations of the carbon fibers, the inherent anisotropic properties of the porous electrodes must be considered. The graded GDL, CL and MPL must be designed along both the through-plane and in-plane directions.

For the GDL and MPL, the distributions of porosity and hydrophobicity are the two most important design parameters. An increase in the GDL porosity and PTFE content from the CL/GDL interface toward the GDL/channel interface along the through-plane direction and from the channel inlet to the outlet in the in-plane direction can improve the cell performance at high current densities. The optimal distribution of porosity within the MPL depends not only on the volume fraction but also on the pore size of the void space. In the case of a large pore size, the decrease of the porosity from the CL/MPL interface to the MPL/GDL interface is helpful in improving the cell performance. However, in the case of a small pore size, the MPL porosity near the MPL/GDL interface should be higher than that near the CL/MPL interface to facilitate liquid water expulsion and reactant gas diffusion. An increase in the PTFE content inside the MPL from the CL/MPL interface toward the MPL/GDL interface could hydrate the membrane by retaining the product water in the CL under low humidity conditions. At high relative humidity, such a gradient is able to remove liquid water from the electrode more effectively.

For the CL, the distributions of ionomer and platinum loadings were mainly investigated. It is commonly accepted that a linear decrease in the ionomer loading from the membrane/CL interface to the CL/GDL interface benefits cell performance. The optimal distributions of Pt loading vary for different conditions. If the reactant gas diffusion is the rate-limiting step, e.g., for a CL with low porosity operating at a high current density, the best cell performance is obtained when more Pt particles are located close to the CL/GDL interface. In contrast, if the ionic ohmic drop becomes the rate limiting step, the performance

is improved by incorporating more Pt particles close to the membrane/CL interface. Along the in-plane direction, increasing the Pt loading along the gas flow direction from the inlet to the outlet is capable of mitigating degradation problems due to the nonuniform current density distribution. The optimal increasing gradient depends on the stoichiometric flow ratio of the reactant gas and GDL porosity.

For a functionally graded membrane, a gradient density of sulfonic acid groups through the membrane thickness is fabricated using irradiation methods. The mechanism of the improved cell performance is better control of the membrane water uptake. The decrease in sulfonic acid sites from the anode to the cathode inside the PEM could prevent the anode from drying out to some extent, thus improving the cell performance.

Owing to the large number of design parameters and the strong interactions between them, the optimization of single parameters alone cannot provide synergetic effects from different parameters. Multivariable optimization is therefore an efficient way to investigate the interrelations between various design parameters and optimize several objectives simultaneously in a fuel cell design.

# 9. Final Discussion and Perspective

Although the graded MEA design is an effective method to improve the cell performance, homogenize the current density and decrease the usage of precious catalyst materials, the drawback of the graded design is the required complexity of MEA preparation and the limited improvement of cell performance at low current densities. The graded design has no effect on the electrochemical kinetics, since the design only reinforces the transport behavior, which plays a more important role in fuel cells operated in medium and high current density ranges than in those operated at low current densities.

The CL and MPL are very thin, at normally a few micrometers in thickness; thus, it is very difficult to control the graded distribution of functional components along through-plane direction in a single-layer CL or MPL using the traditional method. Because of this, a multilayer design has been used in previous

experimental studies. Moreover, the contact resistance between each sublayer would result in extra transport resistance of the species, charge and ions, which was omitted in most experimental works. To fabricate a single-graded CL and MPL, advanced methods and technologies need to be applied in electrode preparation, e.g., a dual-templating approach [112], in situ grown deposition [126-128] and layer-by-layer 3D printing [129]. With respect to modeling activities, the CL morphology is assumed to be constructed by numerous uniformly distributed particles in the majority of the existing models from availableliterature. However, the random distribution and interactions of the functional particles, as well as the possibly of building up effective TPBs, are not considered. For this reason, more precise models based on discrete representation and statistical theory have to be developed, as offered by the Monte Carlo percolation model [130, 131] and by the analytical electrochemical fin model coupled with skeleton-based partitioning [132].

In addition, grading techniques could be used in other PEM-based electrochemical devices, e.g., water electrolyzers and direct methanol fuel cells (DMFC), due to the similarity of their cell structures. Although the cost of PEM fuel cells can be significantly reduced through optimization of the precious metal-based electrode, the development of novel cheap catalyst materials, e.g., modified carbon materials, is considered the eventual solution for PEM fuel cell commercialization and industrialization.

# Acknowledgments

The authors acknowledge the National Natural Science Foundation of China (21522603), the Excellent Youth Foundation of Jiangsu Scientific Committee (BK20140011), the Start-up Fund for Young Researchers of Jiangsu University (16JDG061), the Innovation and Creation Program of Jiangsu province of China (2016-32) and the Natural Scientific Fund of Jiangsu province of China (BK20170530). Grateful acknowledgment is also given to the EPSRC Supergen Fuel Cell Consortium (G030995).

# References

[1] P.N. Pearson, M.R. Palmer, Atmospheric carbon dioxide concentrations over the past 60 million years, *Nature*, **406** (2000) 695-699.

[2] H. Lund, Renewable energy strategies for sustainable development, *Energy*, **32** (2007) 912-919.

[3] X.-P. Zhang, X.-M. Cheng, Energy consumption, carbon emissions, and economic growth in China, *Ecol. Econ.*, **68** (2009) 2706-2712.

[4] M.R. Allen, V.R. Barros, J. Boroome, W. Cramer, R. Christ, *et al.*, Climate Change 2014: Synthesis Report. Contribution of Working Groups I, II and III to the Fifth Assessment Report of the Intergovernmental Panel on Climate Change, Paulina Aldunce, Thomas Downing, Sylvie Joussaume, Zbigniew Kundzewicz, Jean Palutikof et al., ed., Geneva, Switzerland, 2014.

[5] M. Conte, A. Iacobazzi, M. Ronchetti, R. Vellone, Hydrogen economy for a sustainable development: state-of-the-art and technological perspectives, *J. Power Sources*, **100** (2001) 171-187.

[6] Reducing Transport Greenhouse Gas Emissions: Trends adn Data 2010. International transport forum: OECD, 2010. .

[7] D. Das, T.N. Veziroğlu, Hydrogen production by biological processes: a survey of literature, *Int. J. Hydrogen Energy*, **26** (2001) 13-28.

[8] P.P. Edwards, V.L. Kuznetsov, W.I.F. David, N.P. Brandon, Hydrogen and fuel cells: Towards a sustainable energy future, *Energy Policy*, **36** (2008) 4356-4362.

[9] S. Gottesfeld, Fuel cell techno-personal milestones 1984–2006, *J. Power Sources*, **171** (2007) 37-45.

[10] W. Dai, H. Wang, X.-Z. Yuan, J.J. Martin, D. Yang, *et al.*, A review on water balance in the membrane electrode assembly of proton exchange membrane fuel cells, *Int. J. Hydrogen Energy*, **34** (2009) 9461-9478.

[11] Y. Wang, K.S. Chen, J. Mishler, S.C. Cho, X.C. Adroher, A review of polymer electrolyte membrane fuel cells: Technology, applications, and needs on fundamental research, *Appl. Energy*, **88** (2011) 981-1007.

[12] J. Wang, Barriers of scaling-up fuel cells: Cost, durability and reliability, *Energy*, **80** (2015) 509-521.

[13] M. Kawase, K. Sato, R. Mitsui, H. Asonuma, M. Kageyama, K. Yamaguchi, *et al.*, Electrochemical reaction engineering of polymer electrolyte fuel cell, *AIChE J.*, **63** (2017) 249-256.

[14] T. Abdullah, L. Liu, Simulation-based microstructural optimization of solid oxide fuel cell for low temperature operation, *Int. J. Hydrogen Energy*, **41** (2016) 13632-13643.

[15] A. Bertei, A. Barbucci, M.P. Carpanese, M. Viviani, C. Nicolella, Morphological and electrochemical modeling of SOFC composite cathodes with distributed porosity, *Chem. Eng. J.*, **s 207–208** (2012) 167-174.

[16] E.S. Greene, W.K.S. Chiu, M.G. Medeiros, Mass transfer in graded microstructure solid oxide fuel cell electrodes, *J. Power Sources*, **161** (2006) 225-231.

[17] L.C.R. Schneider, C.L. Martin, Y. Bultel, L. Dessemond, D. Bouvard, Percolation effects in functionally graded SOFC electrodes, *Electrochim. Acta*, **52** (2007) 3190-3198.

[18] J. Shi, X. Xue, Bi-functionally Graded Electrode Supported SOFC Modeling and Computational Thermal Fluid Analysis for Experimental Design, *J. Fuel Cell Sci. Technol.*, **8** (2010) 103-110.

[19] T. Zhou, H. Liu, Effects of the electrical resistances of the GDL in a PEM fuel cell, *J. Power Sources*, **161** (2006) 444-453.

[20] H. Meng, A simplified method for solving anisotropic transport phenomena in PEM fuel cells, *J. Power Sources*, **161** (2006) 466-469.

[21] D. Todd, S. Bennett, W. Mérida, Anisotropic electrical resistance of proton exchange membrane fuel cell transport layers as a function of cyclic strain, *Int. J. Hydrogen Energy*, **41** (2016) 6029-6035.

[22] U. Pasaogullari, P.P. Mukherjee, C.-Y. Wang, K.S. Chen, Anisotropic heat and water transport in a PEFC cathode gas diffusion layer, *J. Electrochem. Soc.*, **154** (2007) B823-B834.

[23] C.J. Bapat, S.T. Thynell, Effect of anisotropic thermal conductivity of the GDL and current collector rib width on two-phase transport in a PEM fuel cell, *J. Power Sources*, **179** (2008) 240-251.

[24] J.G. Pharoah, K. Karan, W. Sun, On effective transport coefficients in PEM fuel cell electrodes: Anisotropy of the porous transport layers, *J. Power Sources*, **161** (2006) 214-224.

[25] W.W. Yang, T.S. Zhao, Y.L. He, Modelling of coupled electron and mass transport in anisotropic proton-exchange membrane fuel cell electrodes, *J. Power Sources*, **185** (2008) 765-775.

[26] P. Rama, Y. Liu, R. Chen, H. Ostadi, K. Jiang, *et al.*, A Numerical Study of Structural Change and Anisotropic Permeability in Compressed Carbon Cloth Polymer Electrolyte Fuel Cell Gas Diffusion Layers, *Fuel Cells*, **11** (2011) 274–285.

[27] D.H. Ahmed, H.J. Sung, J. Bae, Effect of GDL permeability on water and thermal management in PEMFCs—I. Isotropic and anisotropic permeability, *Int. J. Hydrogen Energy*, **33** (2008) 3767-3785.

[28] Z. Fishman, J. Hinebaugh, A. Bazylak, Microscale Tomography Investigations of Heterogeneous Porosity Distributions of PEMFC GDLs, *J. Electrochem. Soc.*, **157** (2010) B1643-B1650.

[29] R. Anderson, L. Zhang, Y. Ding, M. Blanco, X. Bi, D. P. Wilkinson, A critical review of two-phase flow in gas flow channels of proton exchange membrane fuel cells. *J. Power Sources*, **195** (2010) 4531-4553.

[30] A. Z. Weber, R. L. Borup, R. M. Darling, P. K. Das, T. J. Dursch, W. Gu et al., A critical review of modeling transport phenomena in polymer electrolyte fuel cells. *J. Electrochem. Soc*., **161** (2014) F1254-F1229.

[31] M. Andersson, S. B. Beale, M. Espinoza, Z. Wu, W. Lehnert, A review of cell-scale multiphase flow modeling, including water management, in polymer electrolyte fuel cells. *Appl. Energy*, **180** (2016) 757-778.

[32] J. H. Nam, M. Kaviany, Effective diffusivity and water-saturation distribution in single- and two-layer PEMFC diffusion medium, *Int. J. Heat Mass Transfer*, **46** (2003) 4595-4611.

[33] M.M. Tomadakis, S.V. Sotirchos, Ordinary and transition regime diffusion in random fiber structures, *AIChE J.*, **39** (1993) 397-412.

[34] M. M. Tomadakis, T. J. Robertson, Viscous permeability of random fiber structures: comparison of electrical and diffusional estimates with experimental and analytical results, *J. Compos. Mater.*, **39** (2005) 163-188.

[35] L. Cindrella, A. M. Kannan, J. F. Lin, K. Saminathan, Y. Ho, C. W. Lin, J. Wertz, J., Gas diffusion layer for proton exchange membrane fuel cells - A review. *J. Power Sources*, **194** (2009) 146-160.

[36] N. Zamel, X. Li, J. Shen, J. Becker, A. Wiegmann, Estimating effective thermal conductivity in carbon paper diffusion media. *Chem. Eng. Sci.*, **65** (2010) 3994-4006.

[37] M. S. Ismail, K. J. Hughes, D. B. Ingham, L. Ma, M. Pourkashanian, Effects of anisotropic permeability and electrical conductivity of gas diffusion layers on the performance of proton exchange membrane fuel cells. *Appl. Energy*, **95** (2012) 50-63.

[38] J. Becker, R. Flückiger, M. Reum, F. N. Büchi, F. Marone, M. Stampanonic, Determination of material properties of gas diffusion layers: experiments and simulations using phase contrast tomographic microscopy. *J. Electrochem. Soc*., **156** (2009) B1175-B1181.

[39] C. Lee, W. Mérida, Gas diffusion layer durability under steady-state and freezing conditions. *J. Power Sources*, **164** (2007) 141-153.

[40] L. Xing, Y. Xu, P. K. Das, B. Mao, Q. Xu, H. Su et al. Numerical matching of anisotropic transport processes in porous electrodes of proton exchange membrane fuel cells. *Chem. Eng. Sci.*, **195** (2019): 127-140.

[41] A. Therdthianwong, P. Manomayidthikarn, S. Therdthianwong, Investigation of membrane electrode assembly (MEA) hot-pressing parameters for proton exchange membrane fuel cell, *Energy*, **32** (2007) 2401-2411.

[42] W. Sun, B.A. Peppley, K. Karan, Modeling the Influence of GDL and flow-field plate parameters on the reaction distribution in the PEMFC cathode catalyst layer, *J. Power Sources*, **144** (2005) 42-53.

[43] C. Lim, C.Y. Wang, Effects of hydrophobic polymer content in GDL on power performance of a PEM fuel cell, *Electrochim. Acta*, **49** (2004) 4149-4156.

[44] P. Rama, Y. Liu, R. Chen, H. Ostadi, K. Jiang, Y. Gao, *et al.*, Simulation of liquid water breakthrough in a nanotomograph reconstrction of a carbon paper gas-diffusion layer, *AIChE J.*, **58** (2012) 646-655.

[45] J.B. Benziger, E. Kimball, R. Mejia-Ariza, I. Kevrekidis, Oxygen mass transport limitations at the cathode of polymer electrolyte membrane fuel cells, *AIChE J.*, **57** (2011) 2505-2517.

[46] H.-S. Chu, C. Yeh, F. Chen, Effects of porosity change of gas diffuser on performance of proton exchange membrane fuel cell, *J. Power Sources*, **123** (2003) 1-9.

[47] R. Roshandel, B. Farhanieh, E. Saievar-Iranizad, The effects of porosity distribution variation on PEM fuel cell performance, *Renew. Energy*, **30** (2005) 1557-1572.

[48] F. Chen, M.-H. Chang, P.-T. Hsieh, Two-phase transport in the cathode gas diffusion layer of PEM fuel cell with a gradient in porosity, *Int. J. Hydrogen Energy*, **33** (2008) 2525-2529.

[49] Y.-X. Huang, C.-H. Cheng, X.-D. Wang, J.-Y. Jang, Effects of porosity gradient in gas diffusion layers on performance of proton exchange membrane fuel cells, *Energy*, **35** (2010) 4786-4794.

[50] Z. Zhan, J. Xiao, D. Li, M. Pan, R. Yuan, Effects of porosity distribution variation on the liquid water flux through gas diffusion layers of PEM fuel cells, *J. Power Sources*, **160** (2006) 1041-1048.

[51] Z. Zhan, J. Xiao, Y. Zhang, M. Pan, R. Yuan, Gas diffusion through differently structured gas diffusion layers of PEM fuel cells, *Int. J. Hydrogen Energy*, **32** (2007) 4443-4451.

[52] P.K. Sinha, C.-Y. Wang, A. Su, Optimization of gas diffusion media for elevated temperature polymer electrolyte fuel cells, *Int. J. Hydrogen Energy*, **32** (2007) 886-894.

[53] Y. Zhang, A. Verma, R. Pitchumani, Optimum design of polymer electrolyte membrane fuel cell with graded porosity gas diffusion layer, *Int. J. Hydrogen Energy*, **41** (2016) 8412-8426.

[54] E. Kimball, T. Whitaker, Y.G. Kevrekidis, J.B. Benziger, Drops, slugs, and flooding in polymer electrolyte membrane fuel cells, *AIChE J.*, **54** (2008) 1313-1332.

[55] J. Lobato, P. Cañizares, M.A. Rodrigo, C. Ruiz-López, J.J. Linares, Influence of the Teflon loading in the gas diffusion layer of PBI-based PEM fuel cells, *J. Appl. Electrochem.*, **38** (2008) 793-802.

[56] J. Ma, Review on Preparation Method of Membrane Electrode Assembly (MEA) for PEMFC, *Prog. Chem.*, **16** (2004) 804-812.

[57] A. Rofaiel, J.S. Ellis, P.R. Challa, A. Bazylak, Heterogeneous through-plane distributions of polytetrafluoroethylene in polymer electrolyte membrane fuel cell gas diffusion layers, *J. Power Sources*, **201** (2012) 219-225.

[58] M. Mathias, J. Roth, J. Fleming, W.L. Lehnert, Handbook of Fuel Cells: Fundamentals, Technology, and Applications, (2003) 1-21.

[59] K. Kang, K. Oh, S. Park, A. Jo, H. Ju, Effect of spatial variation of gas diffusion layer wetting characteristics on through-plane water distribution in a polymer electrolyte fuel cell, *J. Power Sources*, **212** (2012) 93-99.

[60] H. Ito, K. Abe, M. Ishida, A. Nakano, T. Maeda, *et al.*, Effect of through-plane distribution of polytetrafluoroethylene in carbon paper on in-plane gas permeability, *J. Power Sources*, **248** (2014) 822-830.

[61] H. Ito, K. Abe, M. Ishida, C.M. Hwang, A. Nakano, Effect of through-plane polytetrafluoroethylene distribution in a gas diffusion layer on a polymer electrolyte unitized reversible fuel cell, *Int. J. Hydrogen Energy*, **40** (2015) 16556-16565.

[62] H. Ito, T. Iwamura, S. Someya, T. Munakata, A. Nakano, *et al.*, Effect of through-plane polytetrafluoroethylene distribution in gas diffusion layers on performance of proton exchange membrane fuel cells, *J. Power Sources*, **306** (2016) 289-299.

[63] L. Xing, X. Liu, T. Alaje, R. Kumar, M. Mamlouk, *et al.*, A two-phase flow and non-isothermal agglomerate model for a proton exchange membrane (PEM) fuel cell, *Energy*, **73** (2014) 618-634.

[64] L. Xing, M. Mamlouk, R. Kumar, K. Scott, Numerical investigation of the optimal Nafion® ionomer content in cathode catalyst layer: An agglomerate two-phase flow modelling, *Int. J. Hydrogen Energy*, **39** (2014) 9087-9104.

[65] R. Vijay, S.K. Seshadri, P. Haridoss, Gas diffusion layer with PTFE gradients for effective water management in PEM fuel cells, *Trans. Indian Inst. Met.*, **64** (2011) 175-179.

[66] L. Xing, Q. Cai, X. Liu, C. Liu, K. Scott, *et al.*, Anode partial flooding modelling of proton exchange membrane fuel cells: Optimisation of electrode properties and channel geometries, *Chem. Eng. Sci.*, **146** (2016) 88-103.

[67] G.-G. Park, Y.-J. Sohn, T.-H. Yang, Y.-G. Yoon, W.-Y. Lee, *et al.*, Effect of PTFE contents in the gas diffusion media on the performance of PEMFC, *J. Power Sources*, **131** (2004) 182-187.

[68] J.M. Morgan, R. Datta, Understanding the gas diffusion layer in proton exchange membrane fuel cells. I. How its structural characteristics affect diffusion and performance, *J. Power Sources*, **251** (2014) 269-278.

[69] U. Pasaogullari, C.Y. Wang, Two-phase transport and the role of micro-porous layer in polymer electrolyte fuel cells, *Electrochim. Acta*, **49** (2004) 4359-4369.

[70] J.H. Chun, D.H. Jo, S.G. Kim, S.H. Park, C.H. Lee, *et al.*, Development of a porosity-graded micro porous layer using thermal expandable graphite for proton exchange membrane fuel cells, *Renew. Energy*, **58** (2013) 28-33.

[71] H. Tang, S. Wang, M. Pan, R. Yuan, Porosity-graded micro-porous layers for polymer electrolyte membrane fuel cells, *J. Power Sources*, **166** (2007) 41-46.

[72] X. Wang, H. Zhang, J. Zhang, H. Xu, X. Zhu, *et al.*, A bi-functional micro-porous layer with composite carbon black for PEM fuel cells, *J. Power Sources*, **162** (2006) 474-479.

[73] F.-B. Weng, C.-Y. Hsu, M.-C. Su, Experimental study of micro-porous layers for PEMFC with gradient hydrophobicity under various humidity conditions, *Int. J. Hydrogen Energy*, **36** (2011) 13708-13714.

[74] T.E. Springer, Polymer Electrolyte Fuel Cell Model, *J. Electrochem. Soc.*, **138** (1991) 2334-2342.

[75] T. Berning, D.M. Lu, N. Djilali, Three-dimensional computational analysis of transport phenomena in a PEM fuel cell, *J. Power Sources*, **106** (2002) 284-294.

[76] C. Marr, X. Li, Composition and performance modelling of catalyst layer in a proton exchange membrane fuel cell, *J. Power Sources*, **77** (1999) 17-27.

[77] N. Khajeh-Hosseini-Dalasm, M.J. Kermani, D.G. Moghaddam, J.M. Stockie, A parametric study of cathode catalyst layer structural parameters on the performance of a PEM fuel cell, *Int. J. Hydrogen Energy*, **35** (2010) 2417-2427.

[78] D.M. Bernardi, M.W. Verbrugge, A mathematical model of the solid-polymer-electrolyte fuel cell, *J. Electrochem. Soc.*, **139** (1992) 2477-2491.

[79] K. Broka, P. Ekdunge, Modelling the PEM fuel cell cathode, *J. Appl. Electrochem.*, **27** (1997) 281-289.

[80] F.C. Cetinbas, S.G. Advani, A.K. Prasad, A Modified Agglomerate Model with Discrete Catalyst Particles for the PEM Fuel Cell Catalyst Layer, *J. Electrochem. Soc.*, **160** (2013) F750-F756.

[81] W. Sun, B.A. Peppley, K. Karan, An improved two-dimensional agglomerate cathode model to study the influence of catalyst layer structural parameters, *Electrochim. Acta*, **50** (2005) 3359-3374.

[82] F.C. Cetinbas, S.G. Advani, A.K. Prasad, An Improved Agglomerate Model for the PEM Catalyst Layer with Accurate Effective Surface Area Calculation Based on the Sphere-Packing Approach, *J. Electrochem. Soc.*, **161** (2014) F803-F813.

[83] S. Kamarajugadda, S. Mazumder, Numerical investigation of the effect of cathode catalyst layer structure and composition on polymer electrolyte membrane fuel cell performance, *J. Power Sources*, **183** (2008) 629-642.

[84] N. Khajeh-Hosseini-Dalasm, M. Fesanghary, K. Fushinobu, K. Okazaki, A study of the agglomerate catalyst layer for the cathode side of a proton exchange membrane fuel cell: Modeling and optimization, *Electrochim. Acta*, **60** (2012) 55-65.

[85] L. Xing, S. Du, R. Chen, M. Mamlouk, K. Scott, Anode partial flooding modelling of proton exchange membrane fuel cells: Model development and validation, *Energy*, **96** (2016) 80-95.

[86] T. Sousa, M. Mamlouk, K. Scott, A Non-isothermal Model of a Laboratory Intermediate Temperature Fuel Cell Using PBI Doped Phosphoric Acid Membranes, *Fuel Cells*, **10** (2010) 993-1012.

[87] T. Sousa, M. Mamlouk, K. Scott, An isothermal model of a laboratory intermediate temperature fuel cell using PBI doped phosphoric acid membranes, *Chem. Eng. Sci.*, **10** (2010) 2513-2530.

[88] H. Ju, H. Meng, C.Y. Wang, A single-phase, non-isothermal model for PEM fuel cells, *Int. J. Heat Mass Transfer*, **48** (2005) 1303-1315.

[89] A.Z. Weber, Coupled Thermal and Water Management in Polymer Electrolyte Fuel Cells, *J. Electrochem. Soc.*, **153** (2006) A2205-A2214.

[90] M. Uchida, Y. Aoyama, N. Eda, A. Ohta, New Preparation Method for Polymer- Electrolyte Fuel Cells, *J. Electrochem. Soc.*, **142** (1995) 463-468.

[91] M. Uchida, Y. Aoyama, N. Eda, A. Ohta, Investigation of the Microstructure in the Catalyst Layer and Effects of Both Perfluorosulfonate Ionomer and PTFE- Loaded Carbon on the Catalyst Layer of Polymer Electrolyte Fuel Cells, *J. Electrochem. Soc.*, **142** (1995) 4143-4149.

[92] Q. Wang, M. Eikerling, D. Song, Z. Liu, T. Navessin, *et al.*, Functionally Graded Cathode Catalyst Layers for Polymer Electrolyte Fuel Cells: I. Theoretical Modeling, *J. Electrochem. Soc.*, **151** (2004) A950-A957.

[93] Z. Xie, T. Navessin, K. Shi, R. Chow, Q. Wang, *et al.*, Functionally Graded Cathode Catalyst Layers for Polymer Electrolyte Fuel Cells: II. Experimental Study of the Effect of Nafion Distribution, *J. Electrochem. Soc.*, **152** (2005) A1171-A1179.

[94] K.H. Kim, H.J. Kim, K.Y. Lee, J.H. Jang, S.Y. Lee, *et al.*, Effect of Nafion® gradient in dual catalyst layer on proton exchange membrane fuel cell performance, *Int. J. Hydrogen Energy*, **33** (2008) 2783-2789.

[95] H.-N. Su, S.-J. Liao, Y.-N. Wu, Significant improvement in cathode performance for proton exchange membrane fuel cell by a novel double catalyst layer design, *J. Power Sources*, **195** (2010) 3477-3480.

[96] D. Song, Q. Wang, Z. Liu, M. Eikerling, Z. Xie, *et al.*, A method for optimizing distributions of Nafion and Pt in cathode catalyst layers of PEM fuel cells, *Electrochim. Acta*, **50** (2005) 3347-3358.

[97] F. C. Cetinbas, S. G. Advani, A. K. Prasad. Investigation of a polymer electrolyte membrane fuel cell catalyst layer with bidirectionally-graded composition. *J. Power Sources*, **270** (2014): 594-602.

[98] S. Herden, F. Riewald, J. A. Hirschfeld, M. Perchthaler. In-plane structuring of proton exchange membrane fuel cell cathodes: Effect of ionomer equivalent weight structuring on performance and current density distribution, *J. Power Sources*, **355** (2017): 36-43.

[99] O. Antoine, Y. Bultel, P. Ozil, R. Durand, Catalyst gradient for cathode active layer of proton exchange membrane fuel cell, *Electrochim. Acta*, **45** (2000) 4493-4500.

[100] A.D. Taylor, E.Y. Kim, V.P. Humes, J. Kizuka, L.T. Thompson, Inkjet printing of carbon supported platinum 3-D catalyst layers for use in fuel cells, *J. Power Sources*, **171** (2007) 101-106.

[101] H. Matsuda, K. Fushinobu, A. Ohma, K. Okazaki, Structural Effect of Cathode Catalyst Layer on the Performance of PEFC, *J. Therm. Sci. Tech.-JPN*, **6** (2011) 154-163.

[102] O.E. Kongstein, T. Berning, B. Børresen, F. Seland, R. Tunold, Polymer electrolyte fuel cells based on phosphoric acid doped polybenzimidazole (PBI) membranes, *Energy*, **32** (2007) 418-422.

[103] H. Su, H. Liang, B.J. Bladergroen, V. Linkov, B.G. Pollet, *et al.*, Effect of Platinum Distribution in Dual Catalyst Layer Structured Gas Diffusion Electrode on the Performance of High Temperature PEMFC, *J. Electrochem. Soc.*, **161** (2014) F506-F512.

[104] R. Roshandel, F. Ahmadi, Effects of catalyst loading gradient in catalyst layers on performance of polymer electrolyte membrane fuel cells, *Renew. Energy*, **50** (2013) 921-931.

[105] M. Srinivasarao, D. Bhattacharyya, R. Rengaswamy, Optimization studies of a polymer electrolyte membrane fuel cell with multiple catalyst layers, *J. Power Sources*, **206** (2012) 197-203.

[106] L. Xing, W. Shi, P.K. Das, K. Scott, Inhomogeneous distribution of platinum and ionomer in the porous cathode to maximize the performance of a PEM fuel cell, *AIChE J.*, **63** (2017) 4895-4910.

[107] M. Santis, S.A. Freunberger, A. Reiner, F.N. Büchi, Homogenization of the current density in polymer electrolyte fuel cells by in-plane cathode catalyst gradients, *Electrochim. Acta*, **51** (2006) 5383-5393.

[108] M. Prasanna, E.A. Cho, H.J. Kim, I.H. Oh, T.H. Lim, *et al.*, Performance of proton-exchange membrane fuel cells using the catalyst-gradient electrode technique, *J. Power Sources*, **166** (2007) 53-58.

[109] L. Xing, Y. Wang, P. K. Das, K. Scott, W. Shi. Homogenization of current density of PEM fuel cell by in-plane graded distributions of platinum loading and GDL porosity. *Chem. Eng. Sci.*, **192** (2018) 699-713.

[110] S.Y. Lee, H.J. Kim, K.H. Kim, E. Cho, I.H. Oh, *et al.*, Gradient Catalyst Coating for a Proton Exchange Membrane Fuel Cell Operation under Nonhumidified Conditions, *Electrochem. Solid-State Lett.*, **10** (2007) B166-B169.

[111] Z. Penga, I. Pivac, F. Barbir. Experimental validation of varialbe temperature flow field concept for proton exchange membrane fuel cells. Int. J. Hydrogen Energy, **42** (2017) 26084-26093.

[112] M.J. Wang, T. Zhao, W. Luo, Z.X. Mao, S. Chen, W. Ding, *et al.*, Quantified mass transfer and superior antiflooding performance of ordered macro-mesoporous electrocatalysts, *AIChE J.*, **64** (2018) 2881-2889.

[113] Y. Sato, K. Fujii, N. Mitani, A. Matsuura, T. Kakigi, *et al.*, Development of sulfonated FEP–Nafion hybrid proton exchange membranes for PEFC, *Nucl. Instrum. Methods Phys. Res. B*, **265** (2007) 213-216.

[114] H. Fujita, F. Shiraki, Y. Oshima, T. Tatsumi, T. Yoshikawa, *et al.*, The effect of water uptake gradient in membrane electrode assembly on fuel cell performance, *Radiat. Phys. Chem.*, **80** (2011) 201-206.

[115] H. Fujita, F. Shiraki, T. Yoshikawa, Study on Functionally Gradient Proton Exchange Membrane fabricated by EB Irradiation with Heterogeneous Energy Deposition, *J. Photopolym. Sci. Technol.*, **23** (2010) 387-392.

[116] F. Shiraki, T. Yoshikawa, A. Oshima, Y. Oshima, Y. Takasawa, *et al.*, Development of function-graded proton exchange membrane for PEFC using heavy ion beam irradiation, *Nucl. Instrum. Methods Phys. Res. B*, **269** (2011) 1777-1781.

[117] R. Tsuchida, A. Tsukamoto, S. Hiraiwa, A. Oshima, M. Washio, Fabrication of function-graded proton exchange membranes by electron beam irradiation for polymer electrolyte fuel cells under nonhumidified condition, *J. Power Sources*, **240** (2013) 351-358.

[118] A. Verma, R. Pitchumani, Influence of membrane properties on the transient behavior of polymer electrolyte fuel cells, *J. Power Sources*, **268** (2014) 733-743.

[119] A.M. Kannan, L. Cindrella, L. Munukutla, Functionally graded nano-porous gas diffusion layer for proton exchange membrane fuel cells under low relative humidity conditions, *Electrochim. Acta*, **53** (2008) 2416-2422.

[120] D. Song, Q. Wang, Z. Liu, T. Navessin, M. Eikerling, *et al.*, Numerical optimization study of the catalyst layer of PEM fuel cell cathode, *J. Power Sources*, **126** (2004) 104-111.

[121] D. Song, Q. Wang, Z. Liu, T. Navessin, S. Holdcroft, Numerical study of PEM fuel cell cathode with non-uniform catalyst layer, *Electrochim. Acta*, **50** (2004) 731-737.

[122] M. Secanell, R. Songprakorp, A. Suleman, N. Djilali, Multi-objective optimization of a polymer electrolyte fuel cell membrane electrode assembly, *Energy Environ. Sci.*, **1** (2008) 378-388.

[123] M. Secanell, R. Songprakorp, N. Djilali, A. Suleman, Optimization of a proton exchange membrane fuel cell membrane electrode assembly, *Structural & Multidisciplinary Optimization*, **40** (2009) 563-583.

[124] M. Secanell, K. Karan, A. Suleman, N. Djilali, Multi-variable optimization of PEMFC cathodes using an agglomerate model, *Electrochim. Acta*, **52** (2007) 6318-6337.

[125] L. Xing, X. Song, K. Scott, V. Pickert, W. Cao, Multi-variable optimisation of PEMFC cathodes based on surrogate modelling, *Int. J. Hydrogen Energy*, **38** (2013) 14295-14313.

[126] S. Du, B. Millington, B. Pollet. The effect of Nafion ionomer loading coated on gas diffusion electrodes with in-situ grown Pt nanowires and their durability in proton exchange membrane fuel cells. *Int. Hydrogen Energy*, **36** (2011) 4386-4393.

[127] S. Du, K. Lin, S. Malladi, Y. Lu, S. Sun, Q. Xu, R. Steinberger-Wilckens, H. Dong. Plasma nitriding induced growth of Pt-nanowire arrays as high performance elecrocatalysts for fuel cells. *Sci. Rep.* **4** (2014) 6439.

[128] Z. Wei, K. Su, S. Sui, A. He, S. Du. High performance polymer electrolyte membrane fuel cells (PEMFCs) with gradient Pt nanowire cathodes prepared by decal transfer method. *Int. Hydrogen Energy*, **40** (2015) 3068-3074.

[129] J.H. Martin, B.D. Yahata, J.M. Hundley, J.A. Mayer, T.A. Schaedler, T.M. Pollock. 3D printing of high-strength aluminum alloys. *Nature*, **549** (2017) 365-369.

[130] A.S. Martinez, J. Brouwer, Percolation modeling investigation of TPB formation in a solid oxide fuel cell electrode–electrolyte interface, *Electrochim. Acta*, **53** (2008) 3597-3609.

[131] S. Shin, A.-R. Kim, S. Um, Statistical prediction of fuel cell catalyst effectiveness: Quasi-random nano-structural analysis of carbon sphere-supported platinum catalysts, *Int. J. Hydrogen Energy*, **41** (2016) 9507-9520.

[132] A. Nakajo, A.P. Cocco, M.B. DeGostin, A.A. Peracchio, B.N. Cassenti, *et al.*, Accessible triple-phase boundary length: A performance metric to account for transport pathways in heterogeneous electrochemical materials, *J. Power Sources*, **325** (2016) 786-800.

**Figure**

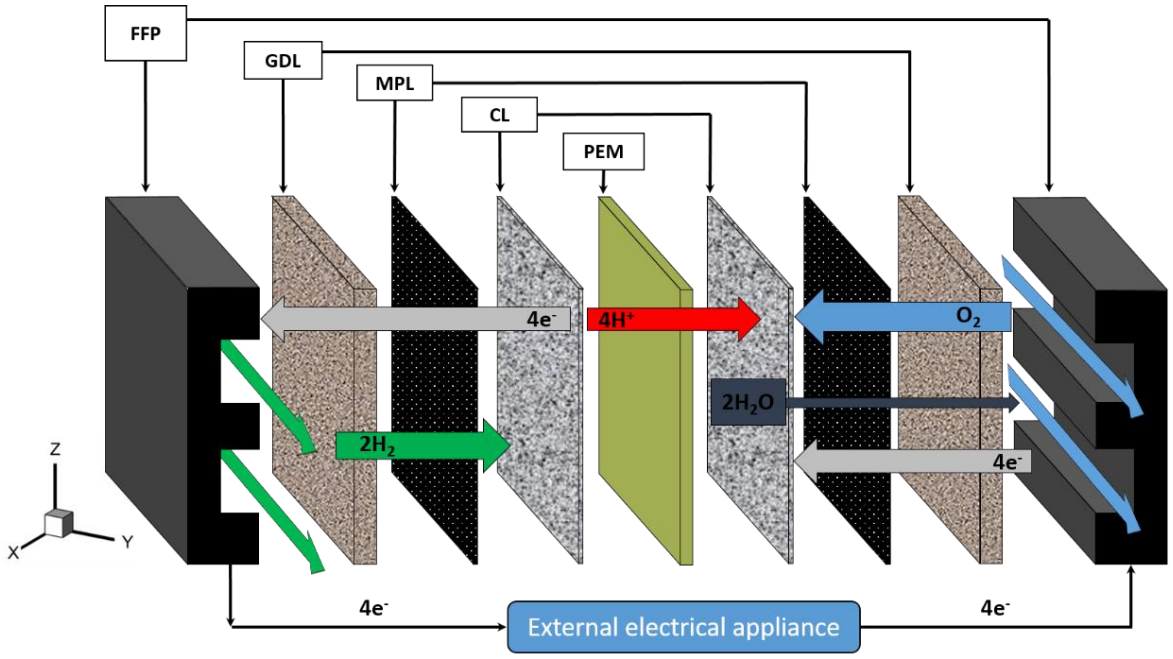


Fig. 1 Layout of a PEM unit and its species, electron and charge transport during operation

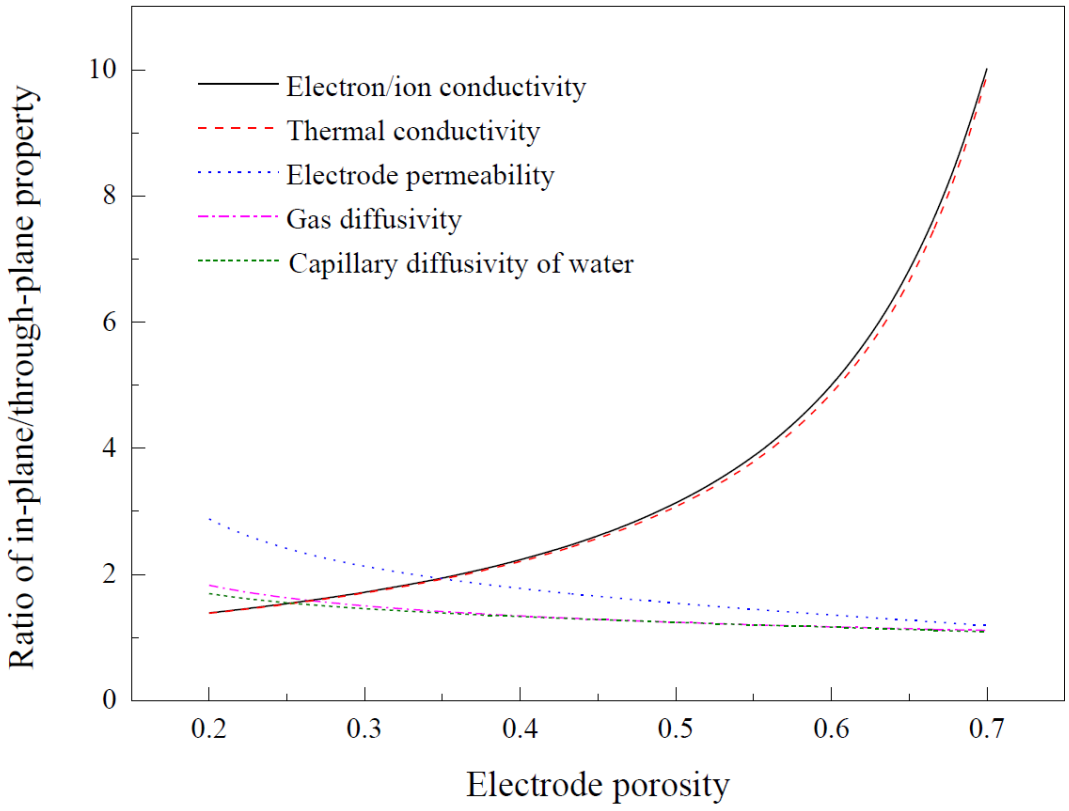


Fig. 2 Ratios of in-plane and through-plane parameters with various electrode porosities [40]

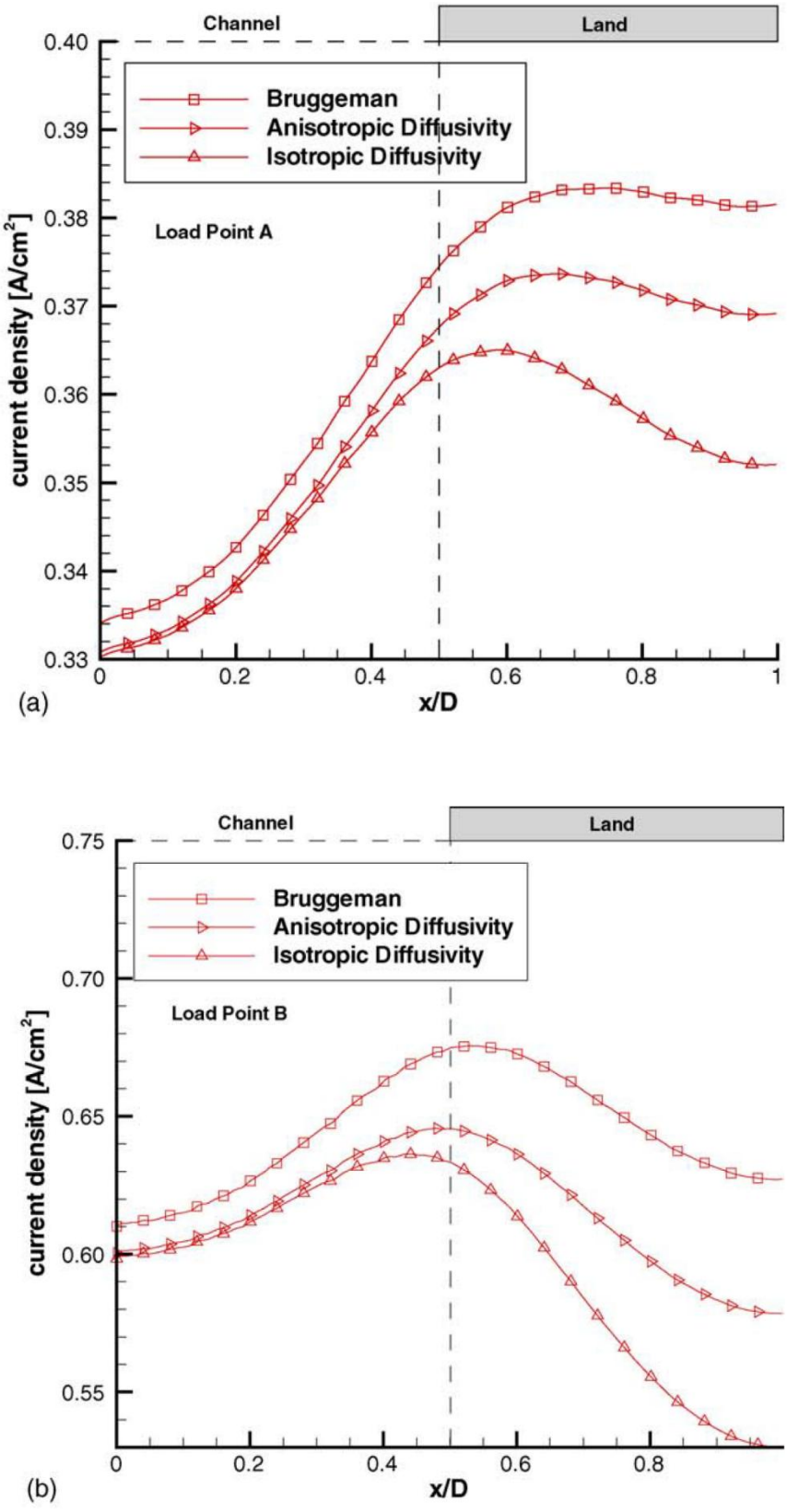


Fig. 3 Distributions of current density around (a) 0.35 and (b) 0.6 A $cm^{-2}$ with anisotropic and isotropic mass diffusivities [24]

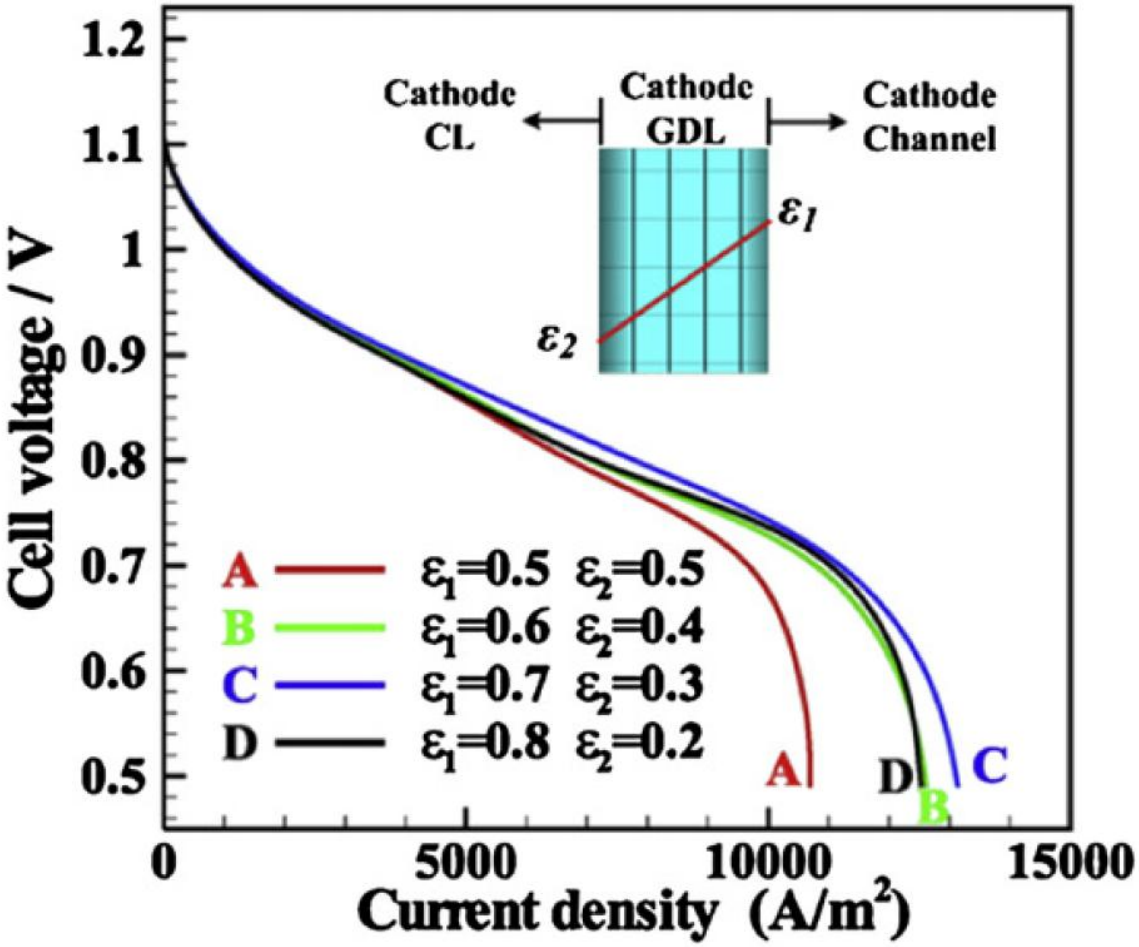


Fig. 4 Predicted cell performance for a porosity-graded cathode GDL with a parallel channel design [49]

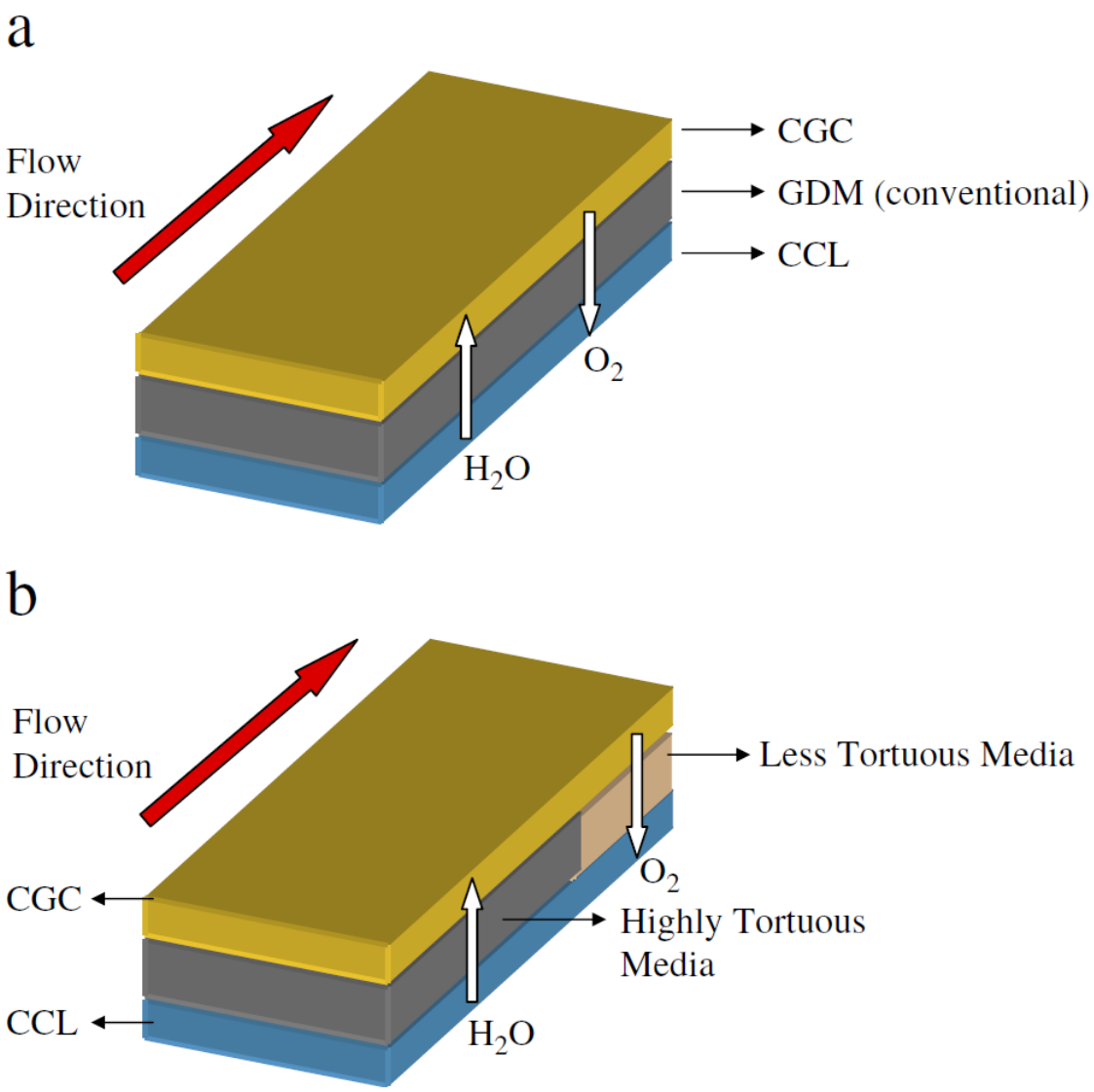


Fig. 5 Schematics of conventional and tortuosity graded diffusion media [52]

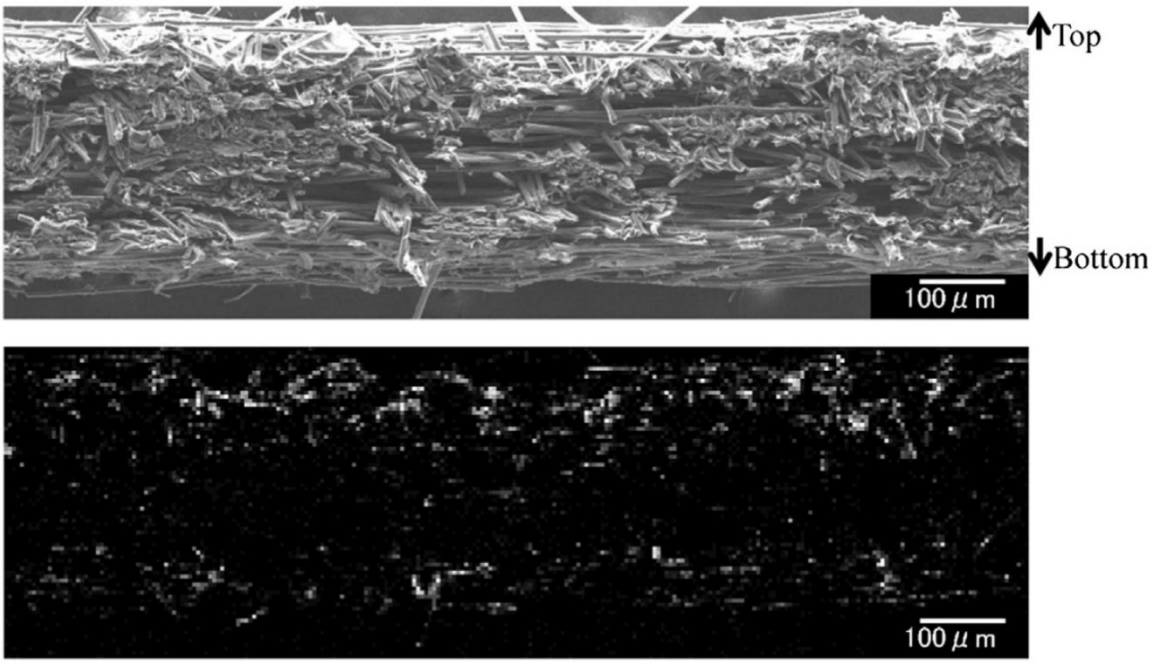


Fig. 6 SEM image and corresponding EDS map of fluorine in the cross-sectional GDL [60]

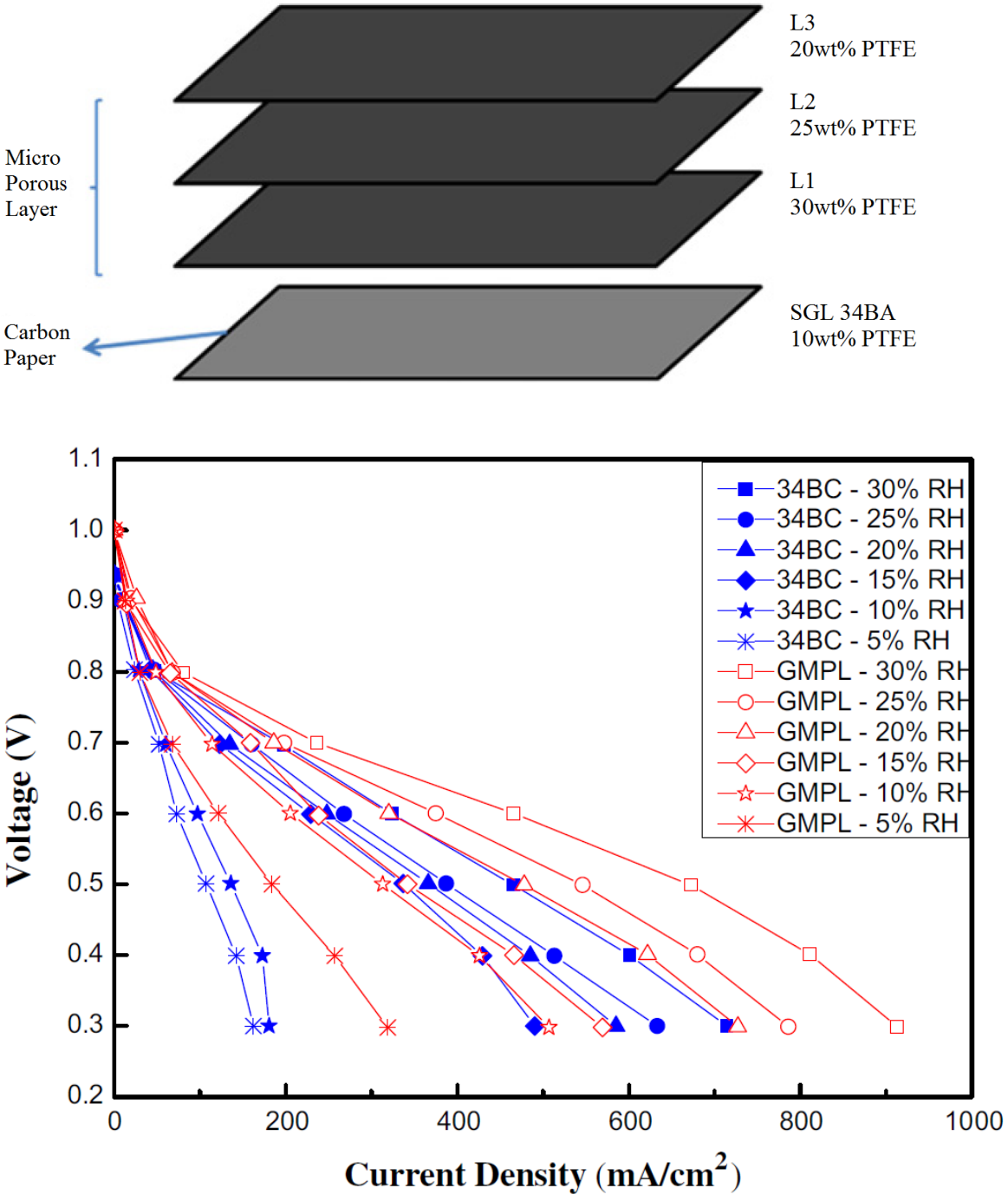


Fig. 7 The cell performance of the commercial MPL (34BC) and GMPL under various relative humidity conditions: the GMPL consists of 34BA (10 wt% PTFE) and three sublayers with various PTFE loadings from 20 to 30 wt% [73]

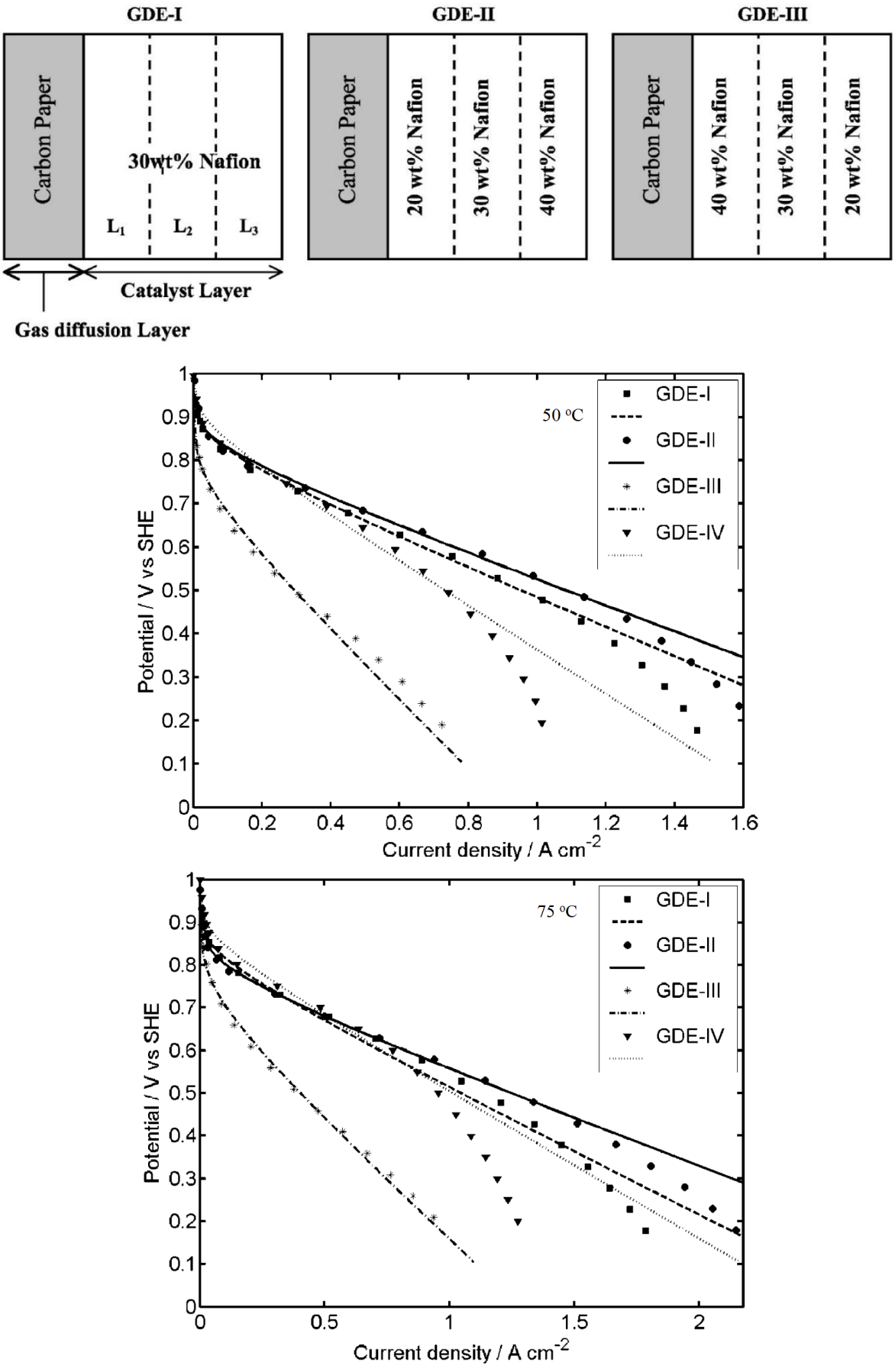


Fig. 8 Graded distribution of Nafion in the cathode CL and the obtained polarization curves [93]

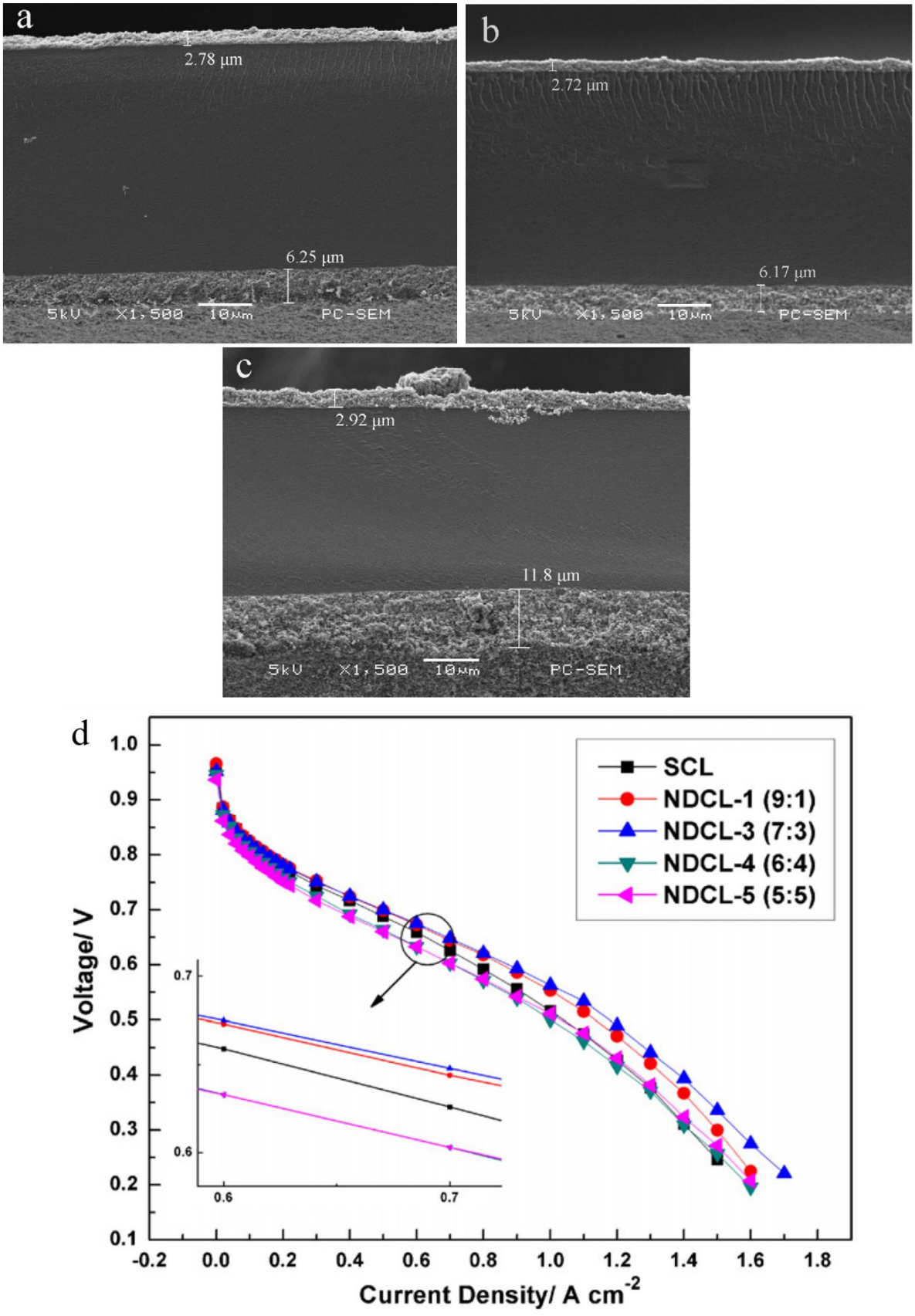


Fig. 9 SEM images of the cross-sectional views of MEAs with (a) SCL (b) DCL and (c) NDCL-2 cathodes and (d) cell performance with various cathode structures [95]

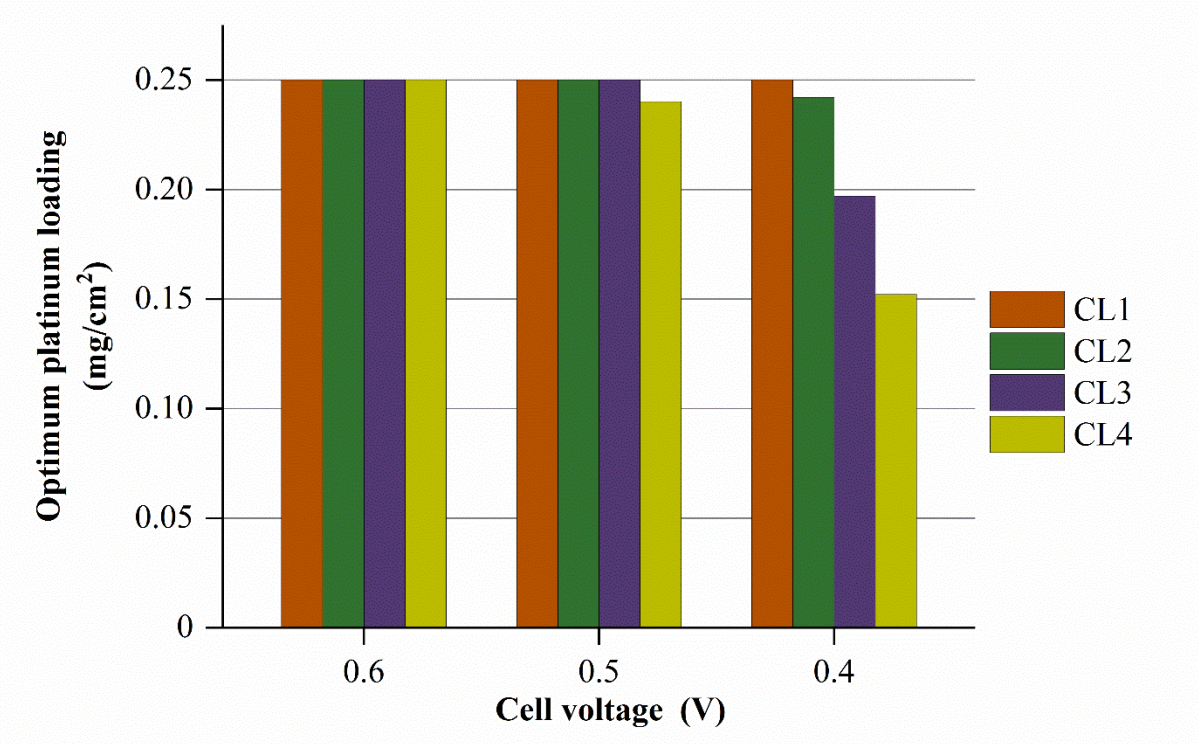


Fig. 10 Optimum distribution of platinum loading in a multilayer CL at various cell voltages: CL1 is the sublayer close to the GDL, and CL4 is the sublayer close to the membrane [105]

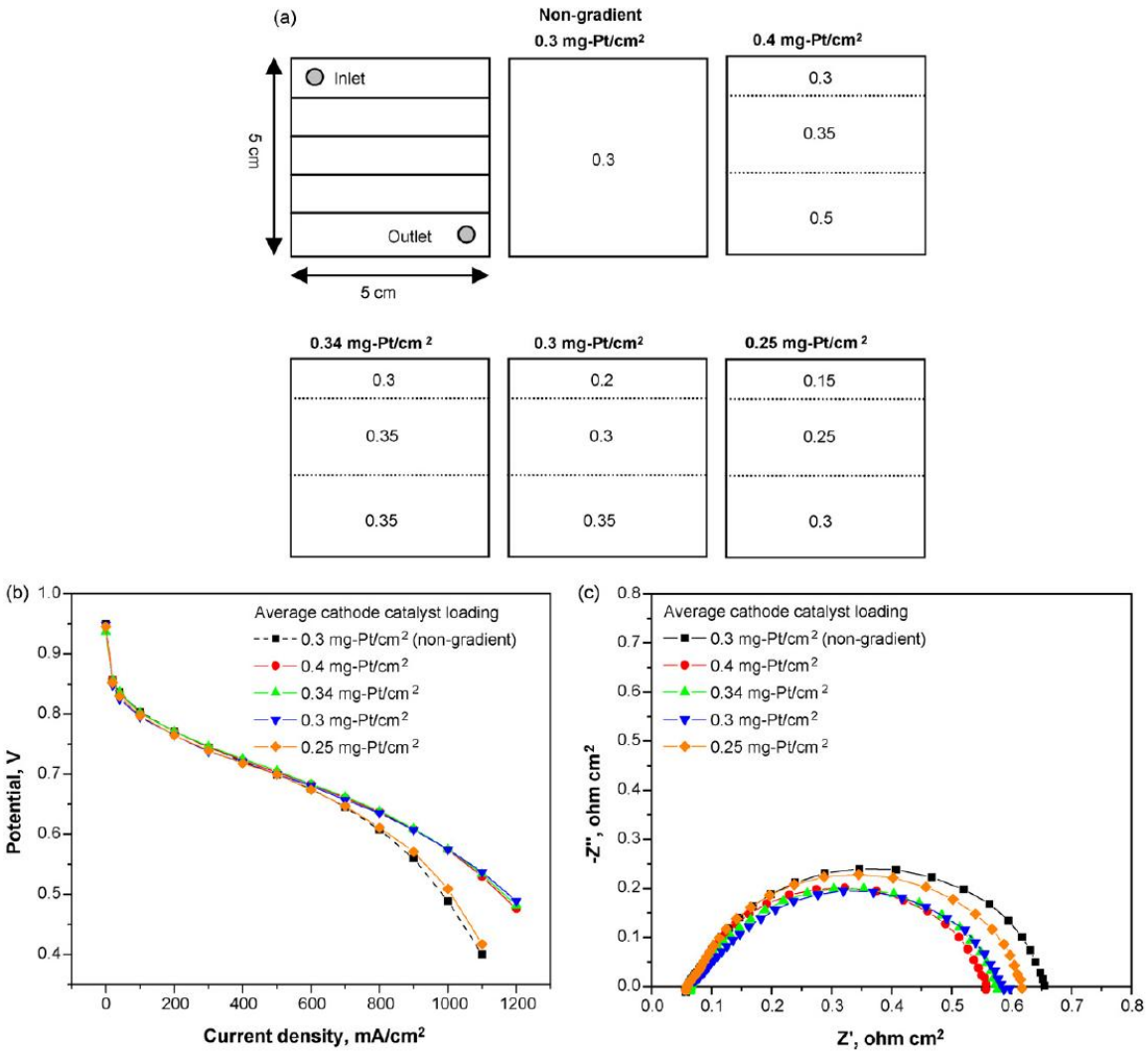


Fig. 11 Effect of the in-plane distribution of platinum on polarization curves and Nyquist plots [108]

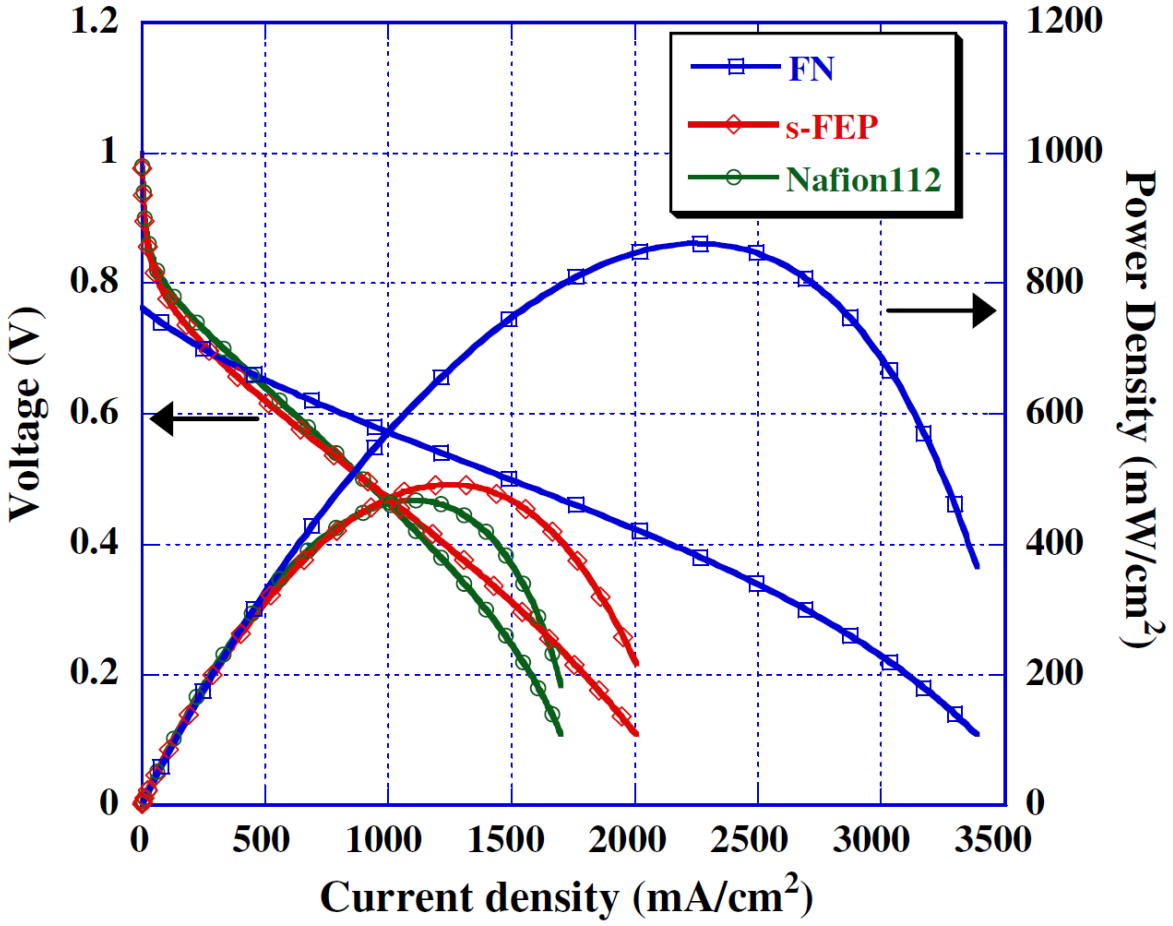


Fig. 12 Cell performances of MEAs based on FN (mixture of radiation-grafted membrane with Nafion ionomer), s-FEP (sulfonated radiation-grafted membrane) and Nafion 112 [113]

**Table**

Table 1 Summary of the graded design of GDL

| Parameter | Grading direction | Optimum distribution profiles and benefits | Experimental or modeling evidence | Reference |
|---|---|---|---|---|
| Porosity | Through-plane | Porosity=exp [$-7.5\times10^{-6}x^2-2.04\times10^{-4}x-0.357$] leads to the highest current density at overpotential of 0.36 V. ($x$ is the GDL thickness). A change in GDL porosity exerts a significant influence in high current density range. | Modeling | 46 |
| | | A gradient in porosity of 80% at GDL-channel boundary and 20% at the CL-GDL boundary benefits the removal rate of liquid water and enhances the transport of oxygen through the cathode GDL. | Modeling | 48 |
| | | A linear porosity gradient with 70% at the GDL-channel boundary and 30% at the CL-GDL boundary increases the limiting current density. | Modeling | 49 |
| | | Porosity=0.4x+0.4 yields the least liquid water and the best cell performance (x is the dimensionless distance through the thickness of the GDL) | Modeling | 50, 51 |
| | In-plane | An optimum value of effective diffusion length of diffusion media is existed for a peak cell performance. A functionally graded diffusion media design can provide a better performance than conventional diffusion media. | Modeling | 52 |
| | | Porosity=$0.16+0.58(L)^{3.02}$ at 0.35 V, and $0.20+0.797(L)^{1.84}$ at 0.5 V (L is the dimensionless channel length along the gas flow direction) improve the uniformity in current density along the length of the channel up to a factor of 10. | Experiment and modeling | 53 |
| Hydrophobicity | Through-plane | A centrally located liquid saturation peaks in the GDLs were explained, which was attributed to relatively fewer PTFE-coated pores in the inner GDL region than in the outer GDL region due to incomplete PTFE treatment. | Modeling | 59 |

| | | | | |
|---|---|---|---|---|
| | | A uniform distribution of PTFE in GDL improved the cell performance under fully humidified condition. The current density at 0.6 V was increased by a factor of about 1.9 in comparison with the non-uniform PEFE distribution. | Experiment | 60 |
| | | The effect of PEFE distribution in the GDL was important even when an MPL was included. The uniform PTFE distribution improved the cell performance at high relative humidity (80-152%) due to the efficient transport of liquid water through the GDL. | Experiment | 61 |
| | | The through-plane PTFE distribution alerted the in-plane gas permeability. The homogeneous distribution of PTFE achieved by the vacuum drying produced a porosity-leveling effect. | Experiment and modeling | 62 |
| | Through-plane and In-plane | The PTFE content near the outlet should be higher along the in-plane direction, because water is prone to accumulate in this region. The manipulation of PTFE gradients were expected to result in effective water management in PEM fuel cells. | Experiment | 65 |

Table 2 Summary of the graded design of MPL

| Parameter | Grading direction | Optimum distribution profiles and benefits | Experimental or modeling evidence | Reference |
|---|---|---|---|---|
| Porosity | Through-plane | The optimal porosity gradually increased from the CL/MPL interface to the gas diffusion backing layer (GDBL)/MPL interface. The single cell performance, especially in high current density region was increased due to the higher water removal ability | Experiment | 70 |
| | | The porosity of the MPL decreased from the inner layer at the CL/MPL interface to the outer layer at the GDL/MPL interface. The graded porosity benefits the cell performance at high current density by facilitating the liquid water transport through large pores and gas diffusion via small pore in the porosity-graded MPL. | Experiment and modeling | 71 |
| | | A MPL with a gradient configuration of 0.7/0.3 (ratio of carbon loading in MPL for CL side and flow filed side), with carbon loadings of 0.7 mg $cm^{-2}$ on the CL side and 0.3 mg $cm^{-2}$ on the flow filed side is preferable for the improved cell performance. | Experiment | 72 |
| Hydrophobicity | | Triple-layer MPL with various PTFE content, 20, 25 and 30 wt% in the MPLs from CL/MPL interface to MPL/GDL interface could retain more water for membrane at low RH and efficiently remove water from electrode at high RH, thus improved the cell performance under both low and high RH conditions. | Experiment | 73 |

Table 3 Summary of the graded design of CL

| Parameter | Grading direction | Optimum distribution profiles and benefits | Experimental or modeling evidence | Reference |
|---|---|---|---|---|
| Ionomer loading | Through-plane | Lower Nafion content of 30 wt% in the GDL side and higher Nafion content of 40 wt% in the membrane side reduced the voltage losses in the CL by 3-5%, and improved the cell performance for intermediate and high current densities. | Modeling and experiment | 92, 93 |
| | | More Nafion ionomer at the inner layer (close to the membrane) and less Nafion ionomer at the outer layer (close to the GDL) achieved improved cell performance at high current densities. | Experiment | 94 |
| | In-plane | Higher Nafion weight ratio under the channel enhanced the ion transport and improved the cell performance. | Modeling | 97 |
| | | Lower equivalent weight of Nafion in the upstream region and higher equivalent weight in the downstream region of reactant gases showed better cell performance and current density uniformity. | Experiment | 98 |
| Pt loading | Through-plane | For diffusion as a rate limiting step, the best performance was obtained by placing more Pt close to the GDL. For ionic ohmic drop as a rate limiting step, the performance was improved when more Pt were located close to the membrane. | Experiment and modeling | 99 |
| | | The highest Pt concentration close to the membrane (50 wt%) while the lowest furthest away (10 wt%) was the optimal distribution for the best cell performance at medium and high current densities. | Experiment | 100 |
| | | For the improved cell performance, the Pt catalyst concentration at the membrane side should be higher at low RH condition. In contrast, the Pt catalyst concentration at the GDL side should be higher at high RH condition. | Modeling and experiment | 101 |

| | | | | |
|---|---|---|---|---|
| | | A double catalyst layer (DCL) with 50 wt% Pt/C close to the membrane and 20 wt% Pt/C near the GDL achieved a maximum power density of 0.83 W $cm^{-2}$ at 0.4 V, that was an improvement compared to the traditional CL. | Experiment | 102 |
| | | PTFE and PVDF based CLs were respectively used as inner and outer layers of the MEA. Pt mass ratio at 3:7 in the inner and outer layers resulted in an improved single cell performance and durability. | Experiment | 103 |
| | | Regardless of the liquid water formation and CL porosity was assumed as 20%, applying more catalyst under the channel and near the membrane-CL interface yielded the improved cell performance. | Modeling | 104 |
| | | Taking the impact of liquid water into account, higher platinum loading near the CL-GDL than that close to the CL-membrane can improve the cell performance by 15% in high current density region and 85% in low current density region. | Modeling | 105 |
| | In-plane | Optimal performance was achieved with lower Pt loading near the inlet and higher near the outlet of the cathode. The optimal gradient of catalyst loading depended on air stoichiometry. | Experiment and modeling | 107 |
| | | For the average Pt loading of 0.3 mg $cm^{-2}$, the optimal Pt loading increased from 0.2 to 0.35 mg $cm^{-2}$, while for the average Pt loading of 0.4 mg $cm^{-2}$, the optimal Pt loading increased from 0.3 to 0.5 mg $cm^{-2}$, from the inlet to the outlet to counteract the depletion of reactants in the gas stream and improve the cell performance. | Experiment | 108 |
| | | Higher amount of Pt catalyst loaded at the cathode inlet, more water was generated at the inlet and the product water was used to hydrate the membrane at nonhumidified condition and improve the cell performance in full range of current density. | Experiment | 109 |
| Pt and ionomer loading | Through-plane | Better cell performance was achieved when Nafion contents in the inner and outer layers were fixed at 33 wt% and 20 wt%. Platinum loading also varies in the two sub-layers, with higher loading in the inner layer and lower loading in the outer layer. | Experiment | 95 |
| | | The optimal distribution of Nafion content is a linearly increasing function in which the content is 23 wt% near the GDL/CL interface and 46 wt% at the CL/membrane interface. However, platinum loading is a convex function, increasing from 0.33 to 0.22 mg $cm^{-2}$ from the GDL/CL interface to the CL/membrane interface. | Modeling | 98 |

Table 4 Summary of the graded design of PEM

| Parameter | Grading direction | Optimum distribution profiles and benefits | Experimental or modeling evidence | Reference |
|---|---|---|---|---|
| Sulfonic acid group | Through-plane | A hybrid MEA was fabricated by coating the mixture of sulfonated FEP powder with Nafion dispersion at the interface between a PEM and electrodes. Cell performance was improved due to the increased ion exchange capacity and water uptake. | Experiment | 112 |
| | | A novel MEA with functionally gradient sulfonated acid group (rich on the anode side) was prepared using low energy EB grafting method. Due to the water uptake gradient, the flooding in the MEA was mitigated and cell performance at high current densities was improved. | Experiment | 113, 114 |
| | | A graded PEM, with more sulfonic acid groups at the anode side, was prepared using a heavy ion beam irradiation. The as-prepared MEA improved the cell performance in terms of voltage stability and durability owing to the better water management. | Experiment | 115 |
| | | Function-graded PEM was compared with traditional Nafion 212 membrane under non-humidified condition. The optimal distribution of the ionic sites is from the anode to the cathode. The cell performance and power density were improved due to the prevention from membrane drying-up. | Experiment | 116 |
| | | A dynamic model for a single channel PEM fuel cell was developed. It suggested that a graded membrane design with decreasing water content across the membrane thickness from the anode to the cathode was a possible approach to prevent the anode dehydration and avoid irreversible damage of the membrane. | Modeling | 117 |